Progress In Electromagnetics Research, Vol. 186, 11–23, 2026

(Received 30 April 2026, Accepted 26 June 2026, Scheduled 6 August 2026)

Green's Matrix and Propagator Matrix for Three-Dimensional Electromagnetic Wave Propagation and Scattering in a Time-Variant Material

Kees Wapenaar* and Evert Slob

Department of Geoscience and Engineering, Delft University of Technology, 2600 GA Delft, The Netherlands

ABSTRACT: Electromagnetic wave propagation and scattering in materials with time-variant parameters are subjects of an active field of research. The theory is usually restricted to transverse-electric or transverse-magnetic modes in one- or two-dimensional settings. Here we discuss the theory of three-dimensional, multi-component electromagnetic waves in a homogeneous, time-variant material. We present 3×3 causal and acausal Green's matrices, and a 6×6 propagator matrix. We derive several fundamental properties such as the conservation of momentum density for a piecewise continuous, time-variant material, symmetry properties of the propagator matrix, and a relation between the causal and acausal Green's matrices. These properties are used in derivation of a general wave-field representation (the counterpart of the Kirchhoff integral for a time-invariant material) and an expression for Green's function retrieval with space correlations (the counterpart of Green's function retrieval with time correlations in a time-invariant material).

1. INTRODUCTION

Electromagnetic waves, propagating through a time-variant material, are scattered when the material parameters suddenly change from one value to another. Research into this phenomenon began in the second half of the last century [1–3] and has developed into a very active field of research since the introduction of dynamic metamaterials [4–10].

The theory for waves in homogeneous, time-variant materials is very similar to that for waves in classical time-invariant, inhomogeneous materials, with the roles of space and time interchanged [3, 11–15]. However, there are important differences. A notable difference is that waves arriving at a time boundary are reflected and transmitted forward in time, whereas waves arriving at a spatial boundary are reflected backward and transmitted forward in space [12–14]. Ref. [16] discusses the consequences for the direction of the wake tail of a two-dimensional impulse response, reflected by a time boundary.

The theory for waves in time-variant materials is usually restricted to transverse-electric (TE) or transverse-magnetic (TM) modes in one-dimensional (1D) or two-dimensional (2D) settings [4, 12, 17–19]. In these situations, the wave field obeys a scalar wave equation, Green's function is a scalar function, and the propagator matrix (also known as the transfer matrix) is a 2×2 matrix. The literature on three-dimensional (3D) waves in time-variant materials is sparse. Refs. [20] and [21] discuss 3D analytical solutions for some specific profiles of time-variant material parameters. Ref. [22] is one of the first studies that presents a more general theory for 3D electromagnetic wave propagation in time-variant materials, including an analysis of operator symmetries.

In this study, we extend our analysis of 2D TE and TM waves [19] to a more general theory for 3D multi-component electromagnetic waves in a homogeneous, time-variant material. Similar to [22], we refrain from considering materials that are simultaneously space- and time-variant (for a discussion of 1D or 2D scalar waves in such materials, see for example [7, 10, 13, 15]). For a 3D homogeneous, time-variant material, the electromagnetic wave field is a 3×1 vector field, obeying a vectorial wave equation (Section 2); Green's function is a 3×3 matrix (Section 3); and the propagator matrix is a 6×6 matrix (Sections 4 and 6). The matrix-vector approach, discussed in Section 4, facilitates the derivation of fundamental properties and relations, such as the conservation of momentum density (Section 5, confirming a result of [22]), the symmetry of the propagator matrix (Section 7), a relation between the Green's matrix and the propagator matrix (Section 8), a relation between the causal and acausal Green's matrices (Section 9), a general wave field representation (Section 10), and an expression for Green's matrix retrieval (Section 11), all for 3D homogeneous, arbitrarily piecewise continuous, time-variant materials.

2. MAXWELL EQUATIONS FOR A 3D TIME-VARIANT MATERIAL

The Maxwell equations for 3D electromagnetic wave propagation read [23, 24]

$$\partial_t \mathbf{D} - \boldsymbol{\nabla} \times \mathbf{H} = -\mathbf{J}^{\mathrm{e}}, \tag{1}$$

$$\partial_t \mathbf{B} + \boldsymbol{\nabla} \times \mathbf{E} = -\mathbf{J}^{\mathrm{m}}. \tag{2}$$

* Corresponding author: Kees Wapenaar (c.p.a.wapenaar@tudelft.nl).

Here, 3×1 vectors $\mathbf{D}(\mathbf{x}, t)$ and $\mathbf{B}(\mathbf{x}, t)$ are the electric and magnetic flux densities, respectively, as a function of the Cartesian coordinate vector $\mathbf{x} = (x, y, z)$ and time t. Vectors $\mathbf{E}(\mathbf{x}, t)$ and $\mathbf{H}(\mathbf{x}, t)$ are the electric and magnetic field strengths, and vectors $\mathbf{J}^{\mathrm{e}}(\mathbf{x}, t)$ and $\mathbf{J}^{\mathrm{m}}(\mathbf{x}, t)$ are the external electric and magnetic current densities. Furthermore, ∂_t stands for the partial differential operator $\frac{\partial}{\partial t}$, and $\boldsymbol{\nabla}$ is the nabla operator, defined as $\boldsymbol{\nabla} = (\partial_x, \partial_y, \partial_z)$.

The wave-field quantities in Equations (1) and (2) are related via the constitutive equations as follows:

$$\mathbf{D} = \varepsilon \mathbf{E}, \tag{3}$$

$$\mathbf{B} = \mu \mathbf{H}, \tag{4}$$

where ε and μ are the permittivity and permeability, respectively, of the material (assuming that the material is instantaneously reacting, and the conductivity is zero). Throughout this paper, we consider a homogeneous, time-variant material; hence, the permittivity and permeability are time-dependent functions: $\varepsilon(t)$ and $\mu(t)$. Whereas for inhomogeneous, time-invariant materials, Equations (3) and (4) are commonly used to eliminate $\mathbf{D}$ and $\mathbf{B}$ from Equations (1) and (2), for homogeneous, time-variant materials, we eliminate $\mathbf{E}$ and $\mathbf{H}$ from these equations [20–22]. This yields

$$\partial_t \mathbf{D} - \frac{1}{\mu(t)} \boldsymbol{\nabla} \times \mathbf{B} = -\mathbf{J}^{\mathrm{e}}, \tag{5}$$

$$\partial_t \mathbf{B} + \frac{1}{\varepsilon(t)} \boldsymbol{\nabla} \times \mathbf{D} = -\mathbf{J}^{\mathrm{m}}. \tag{6}$$

Equations (5) and (6) are valid for continuously varying parameters $\varepsilon(t)$ and $\mu(t)$. For a material with piecewise continuous parameters, Equations (5) and (6) are supplemented with boundary conditions at all time instants where $\varepsilon(t)$ and/or $\mu(t)$ are discontinuous (known as time boundaries). The boundary conditions state that $\mathbf{D}(\mathbf{x}, t)$ and $\mathbf{B}(\mathbf{x}, t)$ are continuous at these time instants [1, 3, 11, 13]. In reality, the parameters do not change instantaneously but transit in a very short time from one value to another. One may treat such a change as a time boundary when the transition time is very small in comparison with the inverse of the dominant frequency.

We obtain a second-order wave equation for the electric flux density $\mathbf{D}$ by eliminating the magnetic flux density $\mathbf{B}$ from Equations (5) and (6). This yields

$$\left(\partial_t \mu \partial_t + \mu c^2 \boldsymbol{\nabla} \times \boldsymbol{\nabla} \times\right) \mathbf{D}(\mathbf{x}, t) = -\partial_t(\mu \mathbf{J}^{\mathrm{e}}) - \boldsymbol{\nabla} \times \mathbf{J}^{\mathrm{m}}, \tag{7}$$

with the time-variant propagation velocity $c(t)$ defined as

$$c = \frac{1}{\sqrt{\mu \varepsilon}}. \tag{8}$$

3. GREEN'S MATRIX

Green's 3×3 matrix $\boldsymbol{\mathcal{G}}(\mathbf{x}, \mathbf{x}_0, t, t_0)$ is introduced as a solution of wave equation (7), with the source vector $-\boldsymbol{\nabla} \times \mathbf{J}^{\mathrm{m}}(\mathbf{x}, t)$ in the right-hand side replaced by a unit source matrix at $\mathbf{x} = \mathbf{x}_0$ and $t = t_0$, that is, $\delta(\mathbf{x} - \mathbf{x}_0)\delta(t - t_0)\mathbf{I}$, and the source vector $\mathbf{J}^{\mathrm{e}}(\mathbf{x}, t)$ set to zero. Hence

$$\left(\partial_t \mu \partial_t + \mu c^2 \boldsymbol{\nabla} \times \boldsymbol{\nabla} \times\right) \boldsymbol{\mathcal{G}}(\mathbf{x}, \mathbf{x}_0, t, t_0) = \delta(\mathbf{x} - \mathbf{x}_0)\delta(t - t_0)\mathbf{I}, \tag{9}$$

with causality condition

$$\boldsymbol{\mathcal{G}}(\mathbf{x}, \mathbf{x}_0, t, t_0) = \mathbf{O}, \quad \text{for} \quad t < t_0. \tag{10}$$

Here, $\mathbf{I}$ and $\mathbf{O}$ are the identity and null matrices, respectively, of appropriate size (here, 3×3). Owing to the causality condition, Green's matrix is non-zero only for $t \geq t_0$, that is, at and after the action of the source at $\mathbf{x} = \mathbf{x}_0$ and $t = t_0$. We partition $\boldsymbol{\mathcal{G}}(\mathbf{x}, \mathbf{x}_0, t, t_0)$ as follows:

$$\boldsymbol{\mathcal{G}}(\mathbf{x}, \mathbf{x}_0, t, t_0) = \begin{pmatrix} \mathcal{G}_{x,x} & \mathcal{G}_{x,y} & \mathcal{G}_{x,z} \\ \mathcal{G}_{y,x} & \mathcal{G}_{y,y} & \mathcal{G}_{y,z} \\ \mathcal{G}_{z,x} & \mathcal{G}_{z,y} & \mathcal{G}_{z,z} \end{pmatrix} (\mathbf{x}, \mathbf{x}_0, t, t_0). \tag{11}$$

Comparing Equation (9) for $\boldsymbol{\mathcal{G}}(\mathbf{x}, \mathbf{x}_0, t, t_0)$ with Equation (7) for $\mathbf{D}(\mathbf{x}, t)$, it is observed that the first subscripts x, y, and z in Equation (11) refer to the components of the $\mathbf{D}$-field at $(\mathbf{x}, t)$, whereas the second subscripts refer to the components of the source at $(\mathbf{x}_0, t_0)$. We illustrate $\mathcal{G}_{x,z}(\mathbf{x}, \mathbf{x}_0, t, t_0)$ with a numerical example in Section 8.

We introduce an acausal Green's matrix $\boldsymbol{\mathcal{G}}^a(\mathbf{x}, \mathbf{x}_0, t, t_0)$, obeying the same wave equation, but with the acausality condition

$$\boldsymbol{\mathcal{G}}^a(\mathbf{x}, \mathbf{x}_0, t, t_0) = \mathbf{O}, \quad \text{for} \quad t > t_0. \tag{12}$$

This acausal Green's matrix is non-zero only for $t \leq t_0$. For increasing t, it propagates towards the singularity at $\mathbf{x} = \mathbf{x}_0$ and $t = t_0$, after which it vanishes. Hence, in this case, the singularity on the right-hand side of Equation (9) acts as a sink. The acausal Green's matrix is partitioned in the same way as the causal Green's matrix, as indicated in Equation (11).

In a general time-variant material, the parameters $\varepsilon(t)$ and $\mu(t)$ for $t \leq t_0$ are unrelated to the parameters for $t \geq t_0$. Consequently, the acausal Green's matrix $\boldsymbol{\mathcal{G}}^a(\mathbf{x}, \mathbf{x}_0, t, t_0)$ propagates through a material different from that for the causal Green's matrix $\boldsymbol{\mathcal{G}}(\mathbf{x}, \mathbf{x}_0, t, t_0)$. Hence, unlike in a time-invariant material, where the acausal Green's function is simply the time-reversal of the causal Green's function (assuming $t_0 = 0$), the acausal Green's matrix $\boldsymbol{\mathcal{G}}^a(\mathbf{x}, \mathbf{x}_0, t, t_0)$ in a time-variant material is not the time-reversal of the causal Green's matrix $\boldsymbol{\mathcal{G}}(\mathbf{x}, \mathbf{x}_0, t, t_0)$. Nevertheless, as we show in Section 9, there exists a relation between causal and acausal Green's matrices, when the source and sink are chosen at different time instants (instead of both at t_0).

Because the causal and acausal Green's matrices $\boldsymbol{\mathcal{G}}(\mathbf{x}, \mathbf{x}_0, t, t_0)$ and $\boldsymbol{\mathcal{G}}^a(\mathbf{x}, \mathbf{x}_0, t, t_0)$ obey the same wave equation with the same singularity on the right-hand side, the difference between these Green's matrices obeys the same wave equation, but with the singularities cancelled. In other words, the homogeneous Green's matrix $\boldsymbol{\mathcal{G}}^h(\mathbf{x}, \mathbf{x}_0, t, t_0)$, defined as

$$\boldsymbol{\mathcal{G}}^h(\mathbf{x}, \mathbf{x}_0, t, t_0) = \boldsymbol{\mathcal{G}}(\mathbf{x}, \mathbf{x}_0, t, t_0) - \boldsymbol{\mathcal{G}}^a(\mathbf{x}, \mathbf{x}_0, t, t_0), \tag{13}$$

obeys the homogeneous wave equation

$$\left(\partial_t \mu \partial_t + \mu c^2 \boldsymbol{\nabla} \times \boldsymbol{\nabla} \times\right) \boldsymbol{\mathcal{G}}^h(\mathbf{x}, \mathbf{x}_0, t, t_0) = \mathbf{O}. \tag{14}$$

Here, "homogeneous" refers to the absence of a singularity on the right-hand side of Equation (14); the material parameters are still (piecewise continuous) functions of t. Finally, note that because we consider homogeneous materials throughout this paper, the Green's matrices are shift-invariant; hence,

$$\boldsymbol{\mathcal{G}}(\mathbf{x},\mathbf{x}_0,t,t_0)=\boldsymbol{\mathcal{G}}(\mathbf{x}-\mathbf{x}_0,\mathbf{0},t,t_0) \tag{15}$$

(where $\mathbf{0}$ is the 3×1 null vector), and similar expressions for $\boldsymbol{\mathcal{G}}^a(\mathbf{x},\mathbf{x}_0,t,t_0)$ and $\boldsymbol{\mathcal{G}}^h(\mathbf{x},\mathbf{x}_0,t,t_0)$.

4. MATRIX-VECTOR WAVE EQUATION

Several authors use a matrix-vector formulation of the wave equation,

$$\partial_t\mathbf{q}=\mathbf{A}\mathbf{q}+\mathbf{d}, \tag{16}$$

to address the time-evolution of waves through a homogeneous, time-variant material [4, 14, 17–19, 25]. In most of these cases, the wave equation is 1D, which means that it accounts for waves propagating along only one space coordinate. In these cases, $\mathbf{q}(x,t)$ in Equation (16) is a 2×1 wave field vector (containing specific components of the $\mathbf{D}$ and $\mathbf{B}$ fields); $\mathbf{d}(x,t)$ is a 2×1 source vector; and $\mathbf{A}(t)$ is a 2×2 operator matrix. In [19], the approach is extended to the 2D situation, with $\mathbf{q}(x,z,t)$ and $\mathbf{d}(x,z,t)$ still being 2×1 vectors and $\mathbf{A}(t)$ a 2×2 operator matrix. This approach addresses, among others, the time evolution of 2D-TE or 2D-TM waves in the x,z-plane. Here, we extend the approach to the 3D situation, with $\mathbf{q}(\mathbf{x},t)$ and $\mathbf{d}(\mathbf{x},t)$ being 6×1 vectors and $\mathbf{A}(t)$ a 6×6 operator matrix. Equations (5) and (6) can be easily captured in the form of Equation (16). To this end, we can use the following definitions:

$$\mathbf{q}=\begin{pmatrix}\mathbf{D}\\ \mathbf{B}\end{pmatrix},\ \mathbf{d}=\begin{pmatrix}-\mathbf{J}^{\mathrm{e}}\\ -\mathbf{J}^{\mathrm{m}}\end{pmatrix},\ \mathbf{A}=\begin{pmatrix}\mathbf{O} & \frac{1}{\mu(t)}\boldsymbol{\nabla}\times\\ -\frac{1}{\varepsilon(t)}\boldsymbol{\nabla}\times & \mathbf{O}\end{pmatrix}, \tag{17}$$

with

$$\boldsymbol{\nabla}\times=\begin{pmatrix}0 & -\partial_z & \partial_y\\ \partial_z & 0 & -\partial_x\\ -\partial_y & \partial_x & 0\end{pmatrix}. \tag{18}$$

With these definitions, Equation (16) can be used as a starting point for modeling the time evolution of $\mathbf{D}(\mathbf{x},t)$ and $\mathbf{B}(\mathbf{x},t)$ through a homogeneous, time-variant material [26]. For a piecewise continuous, time-variant material, Equation (16) is supplemented with boundary conditions, stating that $\mathbf{q}(\mathbf{x},t)$ is continuous at time boundaries (that is, at those time instants where $\varepsilon(t)$ and/or $\mu(t)$ are discontinuous).

However, apart from being a basis for modeling, Equation (16) is also a useful starting point to establish conservation of momentum density (Section 5), to derive a propagator matrix (Section 6) and its symmetry properties (Section 7), to obtain relations for the Green's matrix with the propagator matrix (Section 8) and with the acausal Green's matrix (Section 9), to derive a general wave field representation (Section 10), and an expression for Green's matrix retrieval (Section 11), all for arbitrarily piecewise continuous, time-variant materials. To this end, the operator matrix $\mathbf{A}(t)$ in Equation (16) should, for the 6×6 case, obey the same symmetry property as for the 2×2 case in [19], namely:

$$\mathbf{A}^t\mathbf{N}=-\mathbf{N}\mathbf{A}, \tag{19}$$

where superscript t denotes matrix transposition, and

$$\mathbf{N}=\begin{pmatrix}\mathbf{O} & \mathbf{I}\\ -\mathbf{I} & \mathbf{O}\end{pmatrix}. \tag{20}$$

Unfortunately, operator matrix $\mathbf{A}(t)$, as defined in Equations (17) and (18), does not obey this symmetry property.

To arrive at an alternative definition of operator matrix $\mathbf{A}(t)$ with the desired symmetry property, we first reorganize Equation (6) by applying the operation $-\boldsymbol{\nabla}\times$ to this equation's both sides. By interchanging the order of spatial and temporal differentiation and considering that $\varepsilon(t)$ is independent of $\mathbf{x}$, we obtain

$$\partial_t(-\boldsymbol{\nabla}\times\mathbf{B})-\frac{1}{\varepsilon(t)}\boldsymbol{\nabla}\times\boldsymbol{\nabla}\times\mathbf{D}=\boldsymbol{\nabla}\times\mathbf{J}^{\mathrm{m}}. \tag{21}$$

Equations (5) and (21) can now be captured in the form of Equation (16), with

$$\mathbf{q}\ =\ \begin{pmatrix}\mathbf{D}\\ -\boldsymbol{\nabla}\times\mathbf{B}\end{pmatrix},\quad \mathbf{d}=\begin{pmatrix}-\mathbf{J}^{\mathrm{e}}\\ \boldsymbol{\nabla}\times\mathbf{J}^{\mathrm{m}}\end{pmatrix}, \tag{22}$$

$$\mathbf{A}\ =\ \begin{pmatrix}\mathbf{O} & -\frac{1}{\mu(t)}\mathbf{I}\\ \frac{1}{\varepsilon(t)}\boldsymbol{\nabla}\times\boldsymbol{\nabla}\times & \mathbf{O}\end{pmatrix}, \tag{23}$$

with

$$\boldsymbol{\nabla}\times\boldsymbol{\nabla}\times=\begin{pmatrix}-(\partial_y^2+\partial_z^2) & \partial_x\partial_y & \partial_x\partial_z\\ \partial_x\partial_y & -(\partial_x^2+\partial_z^2) & \partial_y\partial_z\\ \partial_x\partial_z & \partial_y\partial_z & -(\partial_x^2+\partial_y^2)\end{pmatrix}. \tag{24}$$

The operator matrix $\mathbf{A}(t)$, as defined in Equations (23) and (24), obeys the symmetry relation of Equation (19). Furthermore, because $\mathbf{B}(\mathbf{x},t)$ is continuous at a time boundary for all $\mathbf{x}$, its spatial derivatives are also continuous. Hence, the wave field vector $\mathbf{q}(\mathbf{x},t)$, as defined in Equation (22), remains continuous at time boundaries. Note that for the source-free situation we have, according to Equation (5), $\boldsymbol{\nabla}\times\mathbf{B}=\mu\partial_t\mathbf{D}$. Hence, in this case, wave field vector $\mathbf{q}$, as defined in Equation (22), contains the electric flux density $\mathbf{D}$ and its (scaled) first-order time derivative $-\mu\partial_t\mathbf{D}$. In the remainder of this paper, we use the definitions of $\mathbf{q}(\mathbf{x},t)$, $\mathbf{d}(\mathbf{x},t)$ and $\mathbf{A}(t)$, as formulated in Equations (22)–(24).

5. CONSERVATION OF MOMENTUM DENSITY

Because the material parameters $\varepsilon(t)$ and $\mu(t)$ are independent of position $\mathbf{x}$, it is convenient to apply a 3D spatial Fourier transformation to wave equation (16) and analyze this equation in the spatial Fourier domain. Given a space- and time-dependent quantity $f(\mathbf{x},t)$, we define the 3D spatial Fourier transformation as

$$\check{f}(\mathbf{k},t)=\int_{\mathbb{R}^3}f(\mathbf{x},t)\exp(-i\mathbf{k}\cdot\mathbf{x})\mathrm{d}\mathbf{x}, \tag{25}$$

with the wave vector $\mathbf{k}$ defined as $\mathbf{k} = (k_x, k_y, k_z)$. Furthermore, i is the imaginary unit, and $\mathbb{R}$ denotes the set of real numbers. The inverse 3D Fourier transformation is defined as:

$$f(\mathbf{x}, t) = \frac{1}{(2\pi)^3} \int_{\mathbb{R}^3} \check{f}(\mathbf{k}, t) \exp(i\mathbf{k} \cdot \mathbf{x}) \mathrm{d}\mathbf{k}. \tag{26}$$

Note that differentiation with respect to x, y, or z in the space domain is equivalent to multiplication by ik_x, ik_y, or ik_z, respectively, in the spatial Fourier domain. Hence, in the spatial Fourier domain, Equation (16) becomes

$$\partial_t \check{\mathbf{q}} = \check{\mathbf{A}} \check{\mathbf{q}} + \check{\mathbf{d}}, \tag{27}$$

where

$$\check{\mathbf{q}} = \begin{pmatrix} \check{\mathbf{D}} \\ -i\mathbf{k} \times \check{\mathbf{B}} \end{pmatrix}, \quad \check{\mathbf{d}} = \begin{pmatrix} -\check{\mathbf{J}}^{\mathrm{e}} \\ i\mathbf{k} \times \check{\mathbf{J}}^{\mathrm{m}} \end{pmatrix}, \tag{28}$$

$$\check{\mathbf{A}} = \begin{pmatrix} \mathbf{O} & -\frac{1}{\mu(t)}\mathbf{I} \\ -\frac{1}{\varepsilon(t)}\mathbf{k} \times \mathbf{k}\times & \mathbf{O} \end{pmatrix}, \tag{29}$$

with

$$\mathbf{k}\times = \begin{pmatrix} 0 & -k_z & k_y \\ k_z & 0 & -k_x \\ -k_y & k_x & 0 \end{pmatrix}, \tag{30}$$

$$\mathbf{k} \times \mathbf{k}\times = \begin{pmatrix} -(k_y^2 + k_z^2) & k_x k_y & k_x k_z \\ k_x k_y & -(k_x^2 + k_z^2) & k_y k_z \\ k_x k_z & k_y k_z & -(k_x^2 + k_y^2) \end{pmatrix}. \tag{31}$$

Matrix $\check{\mathbf{A}}(\mathbf{k}, t)$, defined in Equations (29) and (31), obeys the same symmetry relation as matrix $\mathbf{A}(t)$, formulated by Equation (19).

We analyze the quantity $\check{\mathbf{q}}^\dagger \mathbf{N} \check{\mathbf{q}}$, where the superscript $\dagger$ denotes transposition and complex conjugation. Using the definitions of $\check{\mathbf{q}}$ and $\mathbf{N}$ and the vector property $\mathbf{a} \cdot (\mathbf{b} \times \mathbf{c}) = (\mathbf{a} \times \mathbf{b}) \cdot \mathbf{c}$, we obtain the following:

$$\begin{aligned} \check{\mathbf{q}}^\dagger \mathbf{N} \check{\mathbf{q}} &= \begin{pmatrix} \check{\mathbf{D}}^\dagger & (-i\mathbf{k} \times \check{\mathbf{B}})^\dagger \end{pmatrix} \begin{pmatrix} \mathbf{O} & \mathbf{I} \\ -\mathbf{I} & \mathbf{O} \end{pmatrix} \begin{pmatrix} \check{\mathbf{D}} \\ -i\mathbf{k} \times \check{\mathbf{B}} \end{pmatrix} \\ &= -i\Big(\check{\mathbf{D}}^* \cdot (\mathbf{k} \times \check{\mathbf{B}}) + (\mathbf{k} \times \check{\mathbf{B}})^* \cdot \check{\mathbf{D}}\Big) \\ &= 2i\Re\Big(\check{\mathbf{D}}^* \cdot (\check{\mathbf{B}} \times \mathbf{k})\Big) = 2i\Re(\check{\mathbf{D}}^* \times \check{\mathbf{B}}) \cdot \mathbf{k}, \end{aligned} \tag{32}$$

where the superscript $*$ denotes complex conjugation, and $\Re$ denotes the real part. Using Equations (3), (4), and (8), the term between brackets in the right-hand side of Equation (32) is related to the Poynting vector $\check{\mathbf{E}}^* \times \check{\mathbf{H}}$ in the $\mathbf{k}, t$-domain as follows:

$$\check{\mathbf{D}}^* \times \check{\mathbf{B}} = \frac{1}{c^2(t)} \check{\mathbf{E}}^* \times \check{\mathbf{H}}. \tag{33}$$

The net power-flux density $\check{\jmath}(\mathbf{k}, t)$ in the direction of the wave vector $\mathbf{k}$ is defined as

$$\check{\jmath}(\mathbf{k}, t) = \frac{1}{2} \Re(\check{\mathbf{E}}^* \times \check{\mathbf{H}}) \cdot \mathbf{n}, \tag{34}$$

with $\mathbf{n} = \mathbf{k}/|\mathbf{k}|$. Similarly, the net momentum density in the same direction is defined as

$$\check{M}(\mathbf{k}, t) = \frac{1}{2} \Re(\check{\mathbf{D}}^* \times \check{\mathbf{B}}) \cdot \mathbf{n} = \frac{1}{c^2(t)} \check{\jmath}(\mathbf{k}, t), \tag{35}$$

[1, 3, 27, 28]. Hence, from Equations (32) and (35), it follows that the analyzed quantity $\check{\mathbf{q}}^\dagger \mathbf{N} \check{\mathbf{q}}$ is proportional to the net momentum density, according to

$$\check{\mathbf{q}}^\dagger \mathbf{N} \check{\mathbf{q}} = 4i|\mathbf{k}| \check{M}(\mathbf{k}, t). \tag{36}$$

We show that the net momentum density $\check{M}(\mathbf{k}, t)$ is conserved in a source-free, piecewise continuous, time-variant material. First, because the wave field vector $\check{\mathbf{q}}$ is continuous at a time boundary, it follows from Equation (36) that $\check{M}(\mathbf{k}, t)$ (for fixed $\mathbf{k}$) is conserved over a time boundary. Next, we analyze $\partial_t(\check{\mathbf{q}}^\dagger \mathbf{N} \check{\mathbf{q}})$ in the source-free situation for the time intervals between the time boundaries. Using Equations (19) and (27) (with $\check{\mathbf{d}} = \mathbf{0}$), noting that $\check{\mathbf{A}}$ is real-valued, we obtain

$$\begin{aligned} \partial_t(\check{\mathbf{q}}^\dagger \mathbf{N} \check{\mathbf{q}}) &= (\partial_t \check{\mathbf{q}}^\dagger) \mathbf{N} \check{\mathbf{q}} + \check{\mathbf{q}}^\dagger \mathbf{N} \partial_t \check{\mathbf{q}} \\ &= \check{\mathbf{q}}^\dagger (\check{\mathbf{A}}^t \mathbf{N} + \mathbf{N} \check{\mathbf{A}}) \check{\mathbf{q}} = 0. \end{aligned} \tag{37}$$

Hence, using Equation (36) we obtain

$$\partial_t \check{M}(\mathbf{k}, t) = 0. \tag{38}$$

This confirms that the net momentum density $\check{M}(\mathbf{k}, t)$ (for fixed $\mathbf{k}$) is a conserved quantity. This is consistent with Reference [22], where momentum conservation is obtained from the continuity equation associated with the Maxwell stress tensor.

Given that $\check{M}(\mathbf{k}, t)$ is conserved, Equation (35) implies that in general the net power-flux density $\check{\jmath}(\mathbf{k}, t)$ is not conserved but varies over time, proportional to $c^2(t)$. This is explained as the result of energy exchange between the wave field and an external source that modulates the material [1, 3, 13].

Finally, note that for point-symmetric wave fields, such as the Green's matrix defined in Section 3, the net momentum density as defined in Equation (35) equals zero for all $\mathbf{k}$ and t, because the momentum of waves propagating in the $\mathbf{k}$-direction is counteracted by that of waves propagating in the opposite direction (the same holds for the net power-flux density as defined in Equation (34)).

6. PROPAGATOR MATRIX

We introduce the 6×6 propagator matrix $\check{\mathbf{W}}(\mathbf{k}, t, t_0)$ (also known as the transfer matrix) for a time-variant material as the solution of the matrix-vector wave equation (27) without the source term [12, 17–19, 25], hence,

$$\partial_t \check{\mathbf{W}} = \check{\mathbf{A}} \check{\mathbf{W}}, \tag{39}$$

with initial condition

$$\check{\mathbf{W}}(\mathbf{k}, t_0, t_0) = \mathbf{I}. \tag{40}$$

Assuming that matrix $\check{\mathbf{W}}(\mathbf{k}, t, t_0)$ is defined in the same time-variant material as wave field vector $\check{\mathbf{q}}(\mathbf{k}, t)$ and that there are no sources for $\check{\mathbf{q}}(\mathbf{k}, t)$ between t_0 and t, we obtain the following representation for $\check{\mathbf{q}}(\mathbf{k}, t)$

$$\check{\mathbf{q}}(\mathbf{k}, t) = \check{\mathbf{W}}(\mathbf{k}, t, t_0) \check{\mathbf{q}}(\mathbf{k}, t_0). \tag{41}$$

This expression shows that matrix $\check{\mathbf{W}}(\mathbf{k}, t, t_0)$ "propagates" the wave field vector $\check{\mathbf{q}}(\mathbf{k}, t_0)$ from t_0 through the time-variant material to t, where t may be larger or smaller than t_0 (and it also holds for $t = t_0$).

By interchanging t_0 and t in Equation (41), we obtain

$$\check{\mathbf{q}}(\mathbf{k}, t_0) = \check{\mathbf{W}}(\mathbf{k}, t_0, t)\check{\mathbf{q}}(\mathbf{k}, t). \tag{42}$$

From Equations (41) and (42), it follows that

$$\check{\mathbf{W}}(\mathbf{k}, t_0, t) = \check{\mathbf{W}}^{-1}(\mathbf{k}, t, t_0). \tag{43}$$

By applying Equation (41) recursively, we find the following recursive expression for $\check{\mathbf{W}}(\mathbf{k}, t_N, t_0)$:

$$\begin{aligned}&\check{\mathbf{W}}(\mathbf{k}, t_N, t_0)\\ &= \check{\mathbf{W}}(\mathbf{k}, t_N, t_{N-1})\cdots\check{\mathbf{W}}(\mathbf{k}, t_n, t_{n-1})\cdots\check{\mathbf{W}}(\mathbf{k}, t_1, t_0),\end{aligned} \tag{44}$$

with $t_1 \cdots t_n \cdots t_{N-1}$ possibly coinciding with the time boundaries. Equations (41) and (44) can be used to model the time evolution of $\check{\mathbf{q}}(\mathbf{k}, t)$ through a piecewise continuous, time-variant material. In Appendix A, we present an explicit expression for $\check{\mathbf{W}}(\mathbf{k}, t_n, t_{n-1})$ for a time-invariant slab. Once $\check{\mathbf{q}}(\mathbf{k}, t)$ is found, we obtain $\mathbf{q}(\mathbf{x}, t)$ by applying the inverse 3D Fourier transformation defined in Equation (26).

7. SYMMETRY PROPERTIES OF PROPAGATOR MATRIX

We derive the symmetry properties of the propagator matrix $\check{\mathbf{W}}(\mathbf{k}, t, t_0)$. To this end, we first show that the product $\check{\mathbf{W}}^t(\mathbf{k}, t, t_0)\mathbf{N}\check{\mathbf{W}}(\mathbf{k}, t, t_N)$ is a propagation invariant, that is, it is independent of t (for fixed t_0 and t_N). Using Equations (19) and (39), we obtain

$$\begin{aligned}&\partial_t\{\check{\mathbf{W}}^t(\mathbf{k}, t, t_0)\mathbf{N}\check{\mathbf{W}}(\mathbf{k}, t, t_N)\}\\ &= \check{\mathbf{W}}^t(\mathbf{k}, t, t_0)\{\check{\mathbf{A}}^t\mathbf{N} + \mathbf{N}\check{\mathbf{A}}\}\check{\mathbf{W}}(\mathbf{k}, t, t_N) = \mathbf{O}.\end{aligned} \tag{45}$$

This confirms that $\check{\mathbf{W}}^t(\mathbf{k}, t, t_0)\mathbf{N}\check{\mathbf{W}}(\mathbf{k}, t, t_N)$ is a propagation invariant.

Next, since this quantity is the same for $t = t_0$ as for $t = t_N$, we obtain

$$\check{\mathbf{W}}^t(\mathbf{k}, t_0, t_0)\mathbf{N}\check{\mathbf{W}}(\mathbf{k}, t_0, t_N) = \check{\mathbf{W}}^t(\mathbf{k}, t_N, t_0)\mathbf{N}\check{\mathbf{W}}(\mathbf{k}, t_N, t_N), \tag{46}$$

or, using Equation (40),

$$\mathbf{N}\check{\mathbf{W}}(\mathbf{k}, t_0, t_N) = \check{\mathbf{W}}^t(\mathbf{k}, t_N, t_0)\mathbf{N}. \tag{47}$$

In Section 11, we use this symmetry relation in derivation of an expression for Green's matrix retrieval.

Using Equation (43), we obtain from Equation (47) (with t_N replaced by t)

$$\mathbf{N}\check{\mathbf{W}}^{-1}(\mathbf{k}, t, t_0) = \check{\mathbf{W}}^t(\mathbf{k}, t, t_0)\mathbf{N}, \tag{48}$$

or, post-multiplying both sides with $\check{\mathbf{W}}(\mathbf{k}, t, t_0)$,

$$\check{\mathbf{W}}^t(\mathbf{k}, t, t_0)\mathbf{N}\check{\mathbf{W}}(\mathbf{k}, t, t_0) = \mathbf{N}. \tag{49}$$

This is a special case of the propagation invariant.

We partition the 6×6 propagator matrix $\check{\mathbf{W}}(\mathbf{k}, t, t_0)$ into four 3×3 submatrices, according to

$$\check{\mathbf{W}}(\mathbf{k}, t, t_0) = \begin{pmatrix}\check{\mathbf{W}}^{D,D} & \check{\mathbf{W}}^{D,B}\\ \check{\mathbf{W}}^{B,D} & \check{\mathbf{W}}^{B,B}\end{pmatrix}(\mathbf{k}, t, t_0). \tag{50}$$

The choice of the superscripts D and B is explained as follows: using Equation (50) in Equation (41), with $\check{\mathbf{q}}(\mathbf{k}, t)$ and $\check{\mathbf{q}}(\mathbf{k}, t_0)$ partitioned as in Equation (28), the first superscripts D and B in Equation (50) refer to the quantities $\check{\mathbf{D}}$ and $-i\mathbf{k}\times\check{\mathbf{B}}$, respectively, in $\check{\mathbf{q}}(\mathbf{k}, t)$, whereas the second superscripts refer to these quantities in $\check{\mathbf{q}}(\mathbf{k}, t_0)$.

With partitioning Equation (50), we obtain from Equation (47) the following symmetry properties for the submatrices:

$$\check{\mathbf{W}}^{D,B}(\mathbf{k}, t_0, t_N) = -\left\{\check{\mathbf{W}}^{D,B}(\mathbf{k}, t_N, t_0)\right\}^t, \tag{51}$$

$$\check{\mathbf{W}}^{B,D}(\mathbf{k}, t_0, t_N) = -\left\{\check{\mathbf{W}}^{B,D}(\mathbf{k}, t_N, t_0)\right\}^t, \tag{52}$$

$$\check{\mathbf{W}}^{B,B}(\mathbf{k}, t_0, t_N) = \left\{\check{\mathbf{W}}^{D,D}(\mathbf{k}, t_N, t_0)\right\}^t. \tag{53}$$

In Section 8, we show that Green's matrix can be expressed in terms of the submatrix $\check{\mathbf{W}}^{D,B}(\mathbf{k}, t, t_0)$. In Section 9, we use the symmetry property of $\check{\mathbf{W}}^{D,B}(\mathbf{k}, t, t_0)$ (Equation (51)) to derive a relation between the causal and acausal Green's matrices.

Next, we show that three of the four submatrices of the propagator matrix can be expressed in terms of the upper-right submatrix $\check{\mathbf{W}}^{D,B}(\mathbf{k}, t, t_0)$. Substituting Equations (29) and (50) into Equation (39), we obtain

$$\check{\mathbf{W}}^{B,B}(\mathbf{k}, t, t_0) = -\mu(t)\partial_t\check{\mathbf{W}}^{D,B}(\mathbf{k}, t, t_0), \tag{54}$$

$$\check{\mathbf{W}}^{B,D}(\mathbf{k}, t, t_0) = -\mu(t)\partial_t\check{\mathbf{W}}^{D,D}(\mathbf{k}, t, t_0). \tag{55}$$

From Equations (53), (54), and (51) we find

$$\check{\mathbf{W}}^{D,D}(\mathbf{k}, t, t_0) = \mu(t_0)\partial_{t_0}\check{\mathbf{W}}^{D,B}(\mathbf{k}, t, t_0). \tag{56}$$

Equations (54) and (56) express $\check{\mathbf{W}}^{B,B}$ and $\check{\mathbf{W}}^{D,D}$ in terms of $\check{\mathbf{W}}^{D,B}$. Finally, we obtain an expression for $\check{\mathbf{W}}^{B,D}$ in terms of $\check{\mathbf{W}}^{D,B}$ by substituting Equation (56) into Equation (55), hence

$$\check{\mathbf{W}}^{B,D}(\mathbf{k}, t, t_0) = -\mu(t)\mu(t_0)\partial_t\partial_{t_0}\check{\mathbf{W}}^{D,B}(\mathbf{k}, t, t_0). \tag{57}$$

In Section 8, we use Equations (54), (56), and (57) to derive relations between the submatrices on the left-hand sides of these equations and Green's matrix.

8. RELATION BETWEEN GREEN'S MATRIX AND PROPAGATOR MATRIX

We show that there are simple relations between the 3×3 Green's matrix, introduced in Section 3, and the 3×3 submatrices of the propagator matrix, introduced in Sections 6 and 7. We start by applying the Fourier transformation, defined in Equation (25), to the wave equation and causality condition for the Green's matrix, given by Equations (9) and (10), respectively. Taking $\mathbf{x}_0 = \mathbf{0}$ and replacing c^2 by $1/\mu\varepsilon$ (Equation (8)), we obtain

$$\left(\partial_t\mu\partial_t - \frac{1}{\varepsilon}\mathbf{k}\times\mathbf{k}\times\right)\check{\boldsymbol{\mathcal{G}}}(\mathbf{k}, \mathbf{0}, t, t_0) = \delta(t - t_0)\mathbf{I}, \tag{58}$$

with causality condition

$$\check{\boldsymbol{\mathcal{G}}}(\mathbf{k}, \mathbf{0}, t, t_0) = \mathbf{O}, \quad \text{for} \quad t < t_0. \tag{59}$$

We show that $\check{\boldsymbol{\mathcal{G}}}(\mathbf{k}, \mathbf{0}, t, t_0)$ is related to submatrix $\check{\mathbf{W}}^{D,B}(\mathbf{k}, t, t_0)$ via

$$\check{\boldsymbol{\mathcal{G}}}(\mathbf{k}, \mathbf{0}, t, t_0) = -H(t - t_0)\check{\mathbf{W}}^{D,B}(\mathbf{k}, t, t_0), \tag{60}$$

where $H(t-t_0)$ is the Heaviside function. Because of this Heaviside function, the causality condition of Equation (59) is fulfilled; therefore it remains to be shown that $-H(t-t_0)\check{\mathbf{W}}^{D,B}(\mathbf{k},t,t_0)$ obeys the same wave equation as $\check{\boldsymbol{\mathcal{G}}}(\mathbf{k},\mathbf{0},t,t_0)$. For the first time derivative, we have

$$\partial_t\{H(t-t_0)\check{\mathbf{W}}^{D,B}(\mathbf{k},t,t_0)\}=\delta(t-t_0)\check{\mathbf{W}}^{D,B}(\mathbf{k},t,t_0)$$
$$+H(t-t_0)\partial_t\check{\mathbf{W}}^{D,B}(\mathbf{k},t,t_0). \tag{61}$$

From Equations (40) and (50), we find $\check{\mathbf{W}}^{D,B}(\mathbf{k},t_0,t_0)=\mathbf{O}$. Using this and Equation (54), we obtain:

$$\partial_t\{H(t-t_0)\check{\mathbf{W}}^{D,B}(\mathbf{k},t,t_0)\}=-\frac{1}{\mu(t)}H(t-t_0)\check{\mathbf{W}}^{B,B}(\mathbf{k},t,t_0). \tag{62}$$

For the second time derivative, we obtain

$$\partial_t\left(\mu(t)\partial_t\{-H(t-t_0)\check{\mathbf{W}}^{D,B}(\mathbf{k},t,t_0)\}\right)$$
$$=\delta(t-t_0)\check{\mathbf{W}}^{B,B}(\mathbf{k},t,t_0)+H(t-t_0)\partial_t\check{\mathbf{W}}^{B,B}(\mathbf{k},t,t_0). \tag{63}$$

From Equations (40) and (50), we find $\check{\mathbf{W}}^{B,B}(\mathbf{k},t_0,t_0)=\mathbf{I}$. Using this and Equations (29), (39), and (50), we obtain

$$\partial_t\left(\mu(t)\partial_t\{-H(t-t_0)\check{\mathbf{W}}^{D,B}(\mathbf{k},t,t_0)\}\right)=\delta(t-t_0)\mathbf{I}$$
$$+\frac{1}{\varepsilon(t)}\mathbf{k}\times\mathbf{k}\times\{-H(t-t_0)\check{\mathbf{W}}^{D,B}(\mathbf{k},t,t_0)\}. \tag{64}$$

This is the wave equation (58), with $\check{\boldsymbol{\mathcal{G}}}(\mathbf{k},\mathbf{0},t,t_0)$ replaced by $-H(t-t_0)\check{\mathbf{W}}^{D,B}(\mathbf{k},t,t_0)$. This completes the proof of Equation (60).

The Fourier transformed acausal Green's matrix $\check{\boldsymbol{\mathcal{G}}}^a(\mathbf{k},\mathbf{0},t,t_0)$ also obeys wave equation (58), but with the acausality condition $\check{\boldsymbol{\mathcal{G}}}^a(\mathbf{k},\mathbf{0},t,t_0)=\mathbf{O}$ for $t>t_0$. Following a similar derivation as above, it follows that $\check{\boldsymbol{\mathcal{G}}}^a(\mathbf{k},\mathbf{0},t,t_0)$ can be expressed, analogous to Equation (60), as

$$\check{\boldsymbol{\mathcal{G}}}^a(\mathbf{k},\mathbf{0},t,t_0)=H(t_0-t)\check{\mathbf{W}}^{D,B}(\mathbf{k},t,t_0). \tag{65}$$

Conversely, by combining Equations (60) and (65), we can express $\check{\mathbf{W}}^{D,B}(\mathbf{k},t,t_0)$ in terms of Green's matrix and its acausal version, according to

$$\check{\mathbf{W}}^{D,B}(\mathbf{k},t,t_0)\;=\;\check{\boldsymbol{\mathcal{G}}}^a(\mathbf{k},\mathbf{0},t,t_0)-\check{\boldsymbol{\mathcal{G}}}(\mathbf{k},\mathbf{0},t,t_0)$$
$$=\;-\check{\boldsymbol{\mathcal{G}}}^h(\mathbf{k},\mathbf{0},t,t_0), \tag{66}$$

where $\check{\boldsymbol{\mathcal{G}}}^h(\mathbf{k},\mathbf{0},t,t_0)$ is the Fourier transform of the homogeneous Green's matrix $\boldsymbol{\mathcal{G}}^h(\mathbf{x},\mathbf{x}_0,t,t_0)$, defined in Equation (13), for $\mathbf{x}_0=\mathbf{0}$. Using Equations (54), (56), and (57), the other submatrices of the propagator matrix $\check{\mathbf{W}}(\mathbf{k},t,t_0)$ can also be expressed in terms of the homogeneous Green's matrix as follows:

$$\check{\mathbf{W}}^{B,B}(\mathbf{k},t,t_0)\;=\;\mu(t)\partial_t\check{\boldsymbol{\mathcal{G}}}^h(\mathbf{k},\mathbf{0},t,t_0), \tag{67}$$

$$\check{\mathbf{W}}^{D,D}(\mathbf{k},t,t_0)\;=\;-\mu(t_0)\partial_{t_0}\check{\boldsymbol{\mathcal{G}}}^h(\mathbf{k},\mathbf{0},t,t_0), \tag{68}$$

$$\check{\mathbf{W}}^{B,D}(\mathbf{k},t,t_0)\;=\;\mu(t)\mu(t_0)\partial_t\partial_{t_0}\check{\boldsymbol{\mathcal{G}}}^h(\mathbf{k},\mathbf{0},t,t_0). \tag{69}$$

Hence, for the 6×6 propagator matrix partitioned as indicated in Equation (50), we obtain

$$\check{\mathbf{W}}(\mathbf{k},t,t_0)=\begin{pmatrix}-\mu(t_0)\partial_{t_0}\check{\boldsymbol{\mathcal{G}}}^h & -\check{\boldsymbol{\mathcal{G}}}^h\\ \mu(t)\mu(t_0)\partial_t\partial_{t_0}\check{\boldsymbol{\mathcal{G}}}^h & \mu(t)\partial_t\check{\boldsymbol{\mathcal{G}}}^h\end{pmatrix}(\mathbf{k},\mathbf{0},t,t_0). \tag{70}$$

Using this relation between the propagator matrix and the Green's matrix, we are now ready to illustrate the Green's matrix for a time-variant material with a numerical example. We consider a homogeneous, piecewise constant material, consisting of four time-independent slabs. The propagation velocities of these slabs are $1.8*10^8$, $2.5*10^8$, $1.5*10^8$, and $1.5*10^8$ m/s, respectively. The permeability is taken constant throughout. The source is chosen at $t_0=0$ ns. The duration of each time slab is 0.25 ns; hence, the time boundaries occur at 0.25, 0.50, and 0.75 ns, respectively (note that at 0.75 ns, there is actually no time boundary, since the velocities of the third and fourth slabs are identical). We use Equation (44) to model the propagator matrix, with time steps $\Delta t_n=t_n-t_{n-1}=0.025$ ns (hence, t_{10}, t_{20}, and t_{30} coincide with aforementioned time boundaries). For $\check{\mathbf{W}}(\mathbf{k},t_n,t_{n-1})$, we use the explicit expression given in Appendix A, where for simplicity, we choose $k_y=0$. After n recursion steps, submatrix $\check{\mathbf{W}}^{D,B}(\mathbf{k},t_n,t_0)$, with $t_n>t_0$, gives, according to Equation (60), minus the Green's matrix $\check{\boldsymbol{\mathcal{G}}}(\mathbf{k},\mathbf{0},t_n,t_0)$, with $\mathbf{k}=(k_x,0,k_z)$. Using the 2D version of the inverse Fourier transformation of Equation (26) to transform this Green's matrix back to the space-time domain yields $\boldsymbol{\mathcal{G}}(\mathbf{x},\mathbf{0},t_n,t_0)$, with $\mathbf{x}=(x,0,z)$, from which the component $\mathcal{G}_{x,z}(\mathbf{x},\mathbf{0},t_n,t_0)$ is selected. It appears that this Green's function has a strong nonpropagating contribution at the source position $\mathbf{x}=\mathbf{0}$, which stems from the term $-k_xk_z\phi_n/(\mu_nc_nk_r^3)=-k_xk_z\Delta t_n/(\mu_nk_r^2)$ in Equation (A5), with $k_r=\sqrt{k_x^2+k_z^2}$. Therefore, instead, we consider submatrix $\check{\mathbf{W}}^{B,D}(\mathbf{k},t_n,t_0)$, with $t_n>t_0$. According to Equation (69), this gives (after inverse Fourier transformation and selection of the x,z-component) $\mu(t_n)\mu(t_0)\partial_{t_n}\partial_{t_0}\mathcal{G}_{x,z}(\mathbf{x},\mathbf{0},t_n,t_0)$. Here, the time-derivatives remove the aforementioned nonpropagating contribution from $\mathcal{G}_{x,z}(\mathbf{x},\mathbf{0},t_n,t_0)$. Figure 1 shows snapshots of this time-differentiated Green's function (convolved with a 2D spatial wavelet with a central wavenumber $k_0/2\pi=100\,\mathrm{m}^{-1}$) for fixed $t_0=0$ ns, as a function of x and z, for $t_1=0.025$, $t_{10}=0.25$, $t_{20}=0.50$, $t_{30}=0.75$, and $t_N=t_{40}=1.00$ ns. Initially, a wave propagates outward from the source at $\mathbf{x}=\mathbf{0}$. The time boundaries at $t_{10}=0.25$ and $t_{20}=0.50$ ns partly transmit and partly reflect the waves. After $t_{20}=0.50$ ns, the waves continue their propagation without further scattering. Note that all snapshots show zero-crossings of the amplitudes at the x- and z-axes. This is typical for the x,z-component of the Green's function, for which the source at $(\mathbf{x}=\mathbf{0},t_0)$ and the receiver at $(\mathbf{x},t_n)$ are mutually perpendicular.

Figure 2 shows cross-sections along the diagonal $x=z$ (avoiding the zero-crossings at the x- and z-axes) of these snapshots, in the form of a d,t-diagram, where $d=\sqrt{x^2+z^2}$ represents the distance to the source. The dashed blue lines correspond to the snapshots in Figure 1 for $t_{10}=0.25$, $t_{20}=0.50$ and $t_{30}=0.75$ ns. This figure clearly shows that transmission

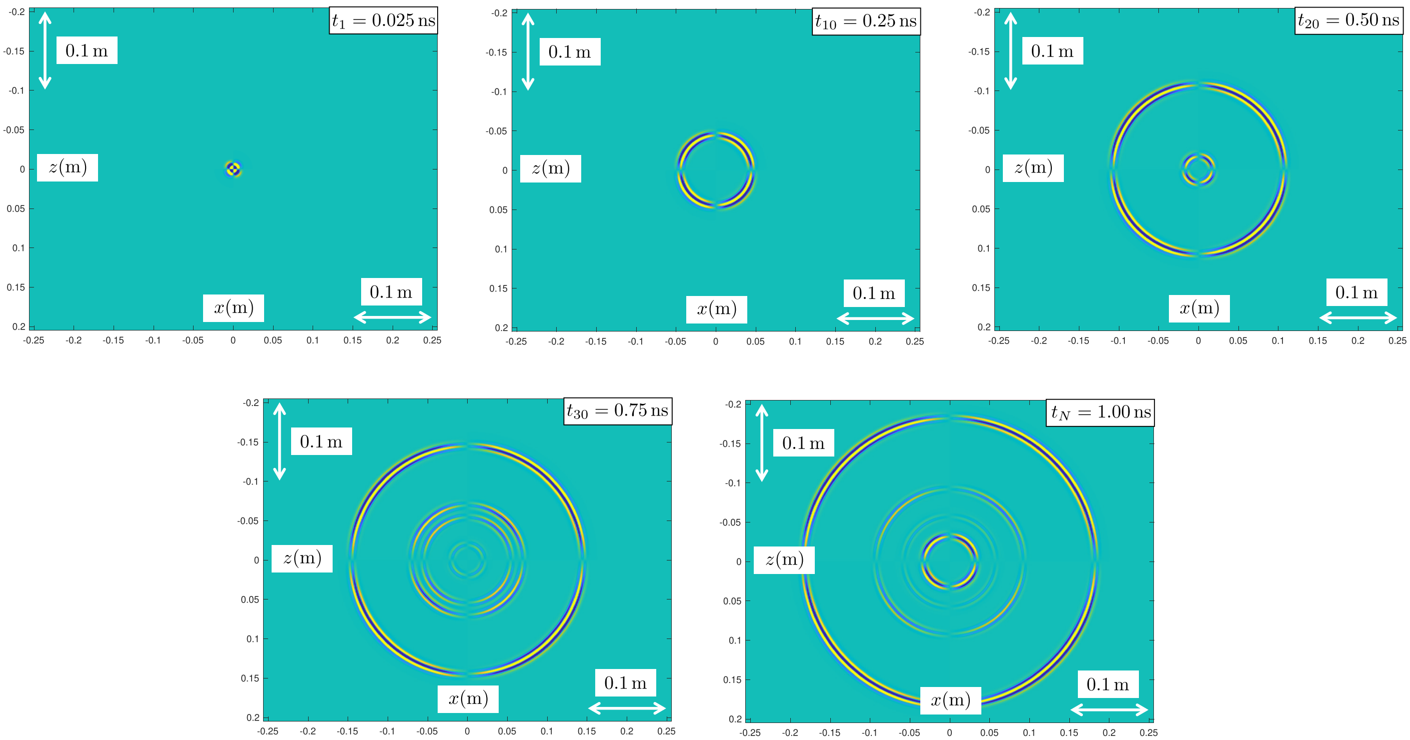

FIGURE 1. Snapshots of the time-differentiated causal Green's function $\mu(t_n)\mu(t_0)\partial_{t_n}\partial_{t_0}\mathcal{G}_{x,z}(\mathbf{x},\mathbf{0},t_n,t_0)$ (convolved with a spatial wavelet) for fixed $t_0 = 0$ ns and variable t_n, for a piecewise constant, time-variant material, with time boundaries at $t_{10} = 0.25$ and $t_{20} = 0.50$ ns. Movie available at https://www.keeswapenaar.nl/TimeMaterial/EMGreenCausal.mp4.

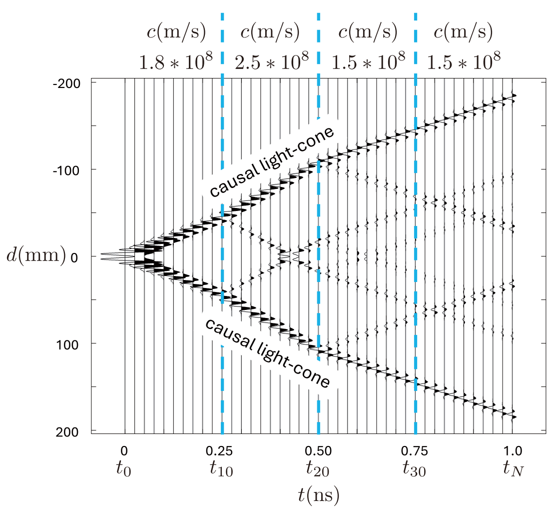

FIGURE 2. Cross-sections along the diagonal $x = z$ of the causal Green's function of Figure 1, with d being the distance to the source, measured along the diagonal.

and reflection occur at the time boundaries indicated by the first two dashed blue lines. Note that the direct outward propagating waves form a "causal light-cone," diverging from the source at $(\mathbf{x} = \mathbf{0}, t_0)$, and that all scattered waves reside inside this cone.

9. RELATION BETWEEN CAUSAL AND ACAUSAL GREEN'S MATRICES

Now that we have expressions for the causal and acausal Green's matrices $\check{\boldsymbol{\mathcal{G}}}(\mathbf{k},\mathbf{0},t,t_0)$ and $\check{\boldsymbol{\mathcal{G}}}^a(\mathbf{k},\mathbf{0},t,t_0)$ in terms of $\check{\mathbf{W}}^{D,B}(\mathbf{k},t,t_0)$ (Equations (60) and (65)), we use the symmetry property of $\check{\mathbf{W}}^{D,B}(\mathbf{k},t,t_0)$ (Equation (51)) to arrive at the following relation between the causal and acausal Green's matrices:

$$\check{\boldsymbol{\mathcal{G}}}^a(\mathbf{k},\mathbf{0},t_0,t_N) = \{\check{\boldsymbol{\mathcal{G}}}(\mathbf{k},\mathbf{0},t_N,t_0)\}^t. \tag{71}$$

Transformed back to the space-time domain, using Equation (26), this gives

$$\boldsymbol{\mathcal{G}}^a(\mathbf{x},\mathbf{0},t_0,t_N) = \{\boldsymbol{\mathcal{G}}(\mathbf{x},\mathbf{0},t_N,t_0)\}^t. \tag{72}$$

For $t_N > t_0$, the causal Green's matrix on the right-hand side is the response to a unit source at $\mathbf{x} = \mathbf{0}$ and $t = t_0$, observed at $\mathbf{x}$ and $t = t_N$. The acausal Green's matrix on the left-hand side is a field observed at $\mathbf{x}$ and $t = t_0$, propagating to a sink at $\mathbf{x} = \mathbf{0}$ and $t = t_N$. For $t_N < t_0$, Equation (72) reduces to the trivial relation $\mathbf{O} = \mathbf{O}$, which follows from Equations (10) and (12).

Similarly, from Equations (51) and (66), we obtain for the homogeneous Green's matrix

$$-\check{\boldsymbol{\mathcal{G}}}^h(\mathbf{k},\mathbf{0},t_0,t_N) = \left\{\check{\boldsymbol{\mathcal{G}}}^h(\mathbf{k},\mathbf{0},t_N,t_0)\right\}^t, \tag{73}$$

or in the space-time domain

$$-\boldsymbol{\mathcal{G}}^h(\mathbf{x},\mathbf{0},t_0,t_N) = \left\{\boldsymbol{\mathcal{G}}^h(\mathbf{x},\mathbf{0},t_N,t_0)\right\}^t. \tag{74}$$

Using the definition of $\boldsymbol{\mathcal{G}}^h(\mathbf{x},\mathbf{0},t_N,t_0)$ in Equation (13), it follows that Equation (72) is a special case of Equation (74) for $t_N > t_0$.

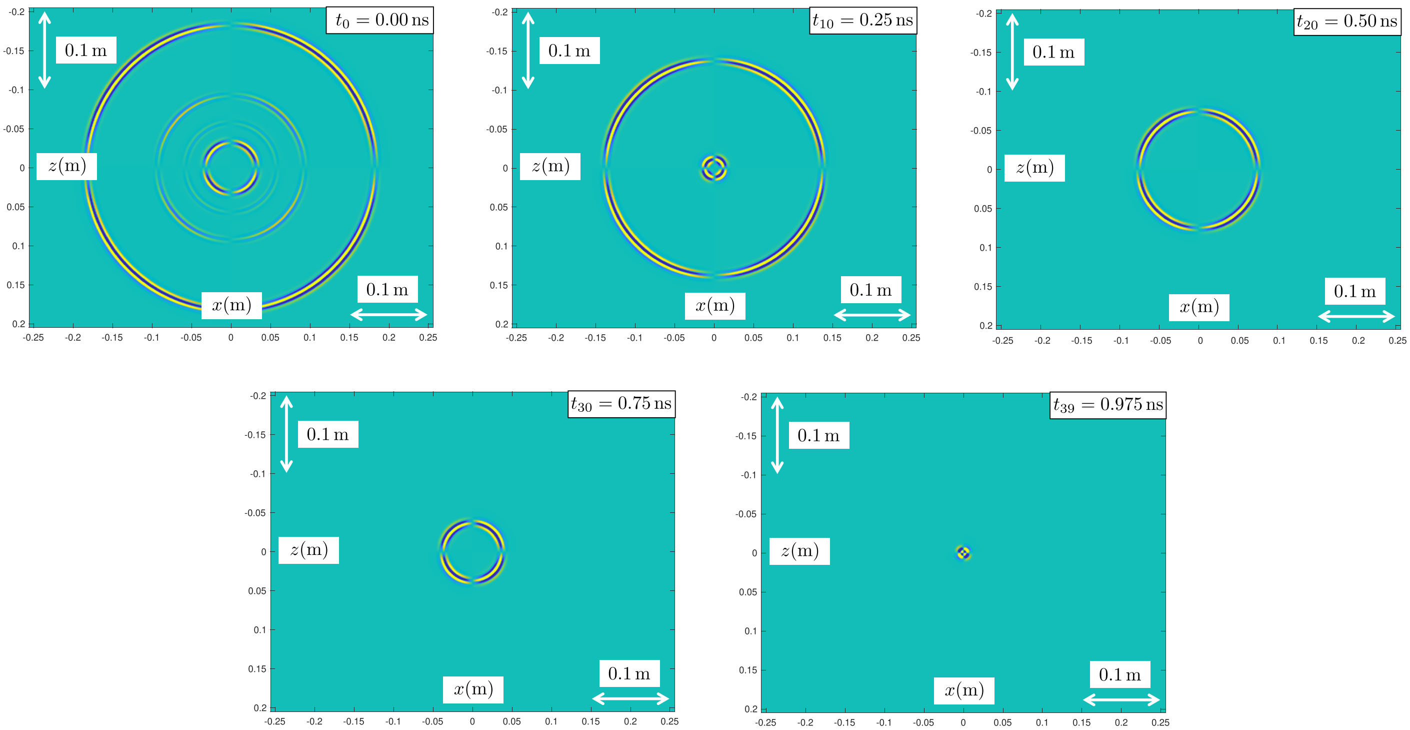

FIGURE 3. Snapshots of the time-differentiated acausal Green's function $\mu(t_n)\mu(t_N)\partial_{t_n}\partial_{t_N}\mathcal{G}^a_{z,x}(\mathbf{x},\mathbf{0},t_n,t_N)$ (convolved with a spatial wavelet) for fixed $t_N = 1.0\,\mathrm{ns}$ and variable t_n, for the same piecewise constant, time-variant material as in Figures 1 and 2. Movie available at https://www.keeswapenaar.nl/TimeMaterial/EMGreenAcausal.mp4.

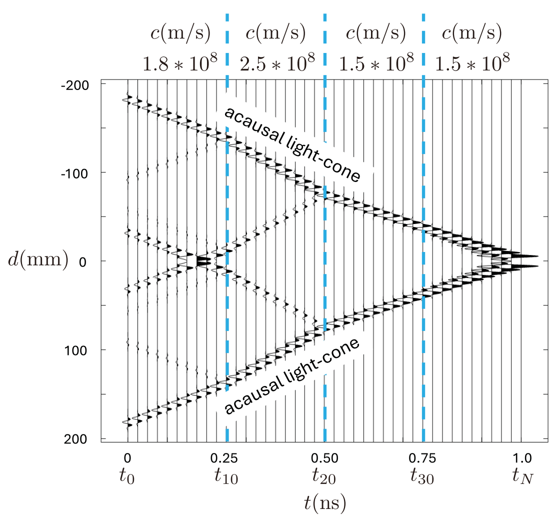

FIGURE 4. Cross-sections along the diagonal $x = z$ of the acausal Green's function of Figure 3.

To illustrate Equation (72) (for the non-trivial situation $t_N > t_0$), we select the x, z-component of the causal Green's matrix. Considering the transposition on the right-hand side of Equation (72), we obtain

$$\mathcal{G}^a_{z,x}(\mathbf{x},\mathbf{0},t_0,t_N) = \mathcal{G}_{x,z}(\mathbf{x},\mathbf{0},t_N,t_0), \tag{75}$$

or, for the time-differentiated versions of these Green's functions,

$$\begin{aligned}&\mu(t_0)\mu(t_N)\partial_{t_0}\partial_{t_N}\mathcal{G}^a_{z,x}(\mathbf{x},\mathbf{0},t_0,t_N)\\ =\ &\mu(t_N)\mu(t_0)\partial_{t_N}\partial_{t_0}\mathcal{G}_{x,z}(\mathbf{x},\mathbf{0},t_N,t_0).\end{aligned} \tag{76}$$

The causal Green's function $\mu(t_n)\mu(t_0)\partial_{t_n}\partial_{t_0}\mathcal{G}_{x,z}(\mathbf{x},\mathbf{0},t_n,t_0)$ (for fixed $t_0 = 0\,\mathrm{ns}$ and variable t_n) is shown in Figures 1 and 2. Similarly, we illustrate the acausal Green's function $\mu(t_n)\mu(t_N)\partial_{t_n}\partial_{t_N}\mathcal{G}^a_{z,x}(\mathbf{x},\mathbf{0},t_n,t_N)$ (for fixed $t_N = 1.0\,\mathrm{ns}$ and variable t_n) in Figures 3 and 4. The latter figure shows that the direct inward-propagating waves form an "acausal light-cone," converging to the sink at $\mathbf{x} = \mathbf{0}$ and $t = t_N$, and that all scattered waves reside inside this cone. According to Equation (76), the acausal Green's function for $t_n = t_0$ (the first snapshot in Figure 3 and the first trace in Figure 4) is identical to the causal Green's function for $t_n = t_N$ (the last snapshot in Figure 1 and the last trace in Figure 2). Note that for all other t_n between t_0 and t_N, the time-dependent behavior of the acausal Green's function (Figures 3 and 4) is, after time-reversal, different from that of the causal Green's function (Figures 1 and 2). This is because the time-variant material between t_0 and t_N is asymmetric. For the special case of a symmetric time-variant material between t_0 and t_N, the time-reversal of the acausal Green's function (shifted over $t_0 + t_N$) is identical to the causal Green's function for all t_n between t_0 and t_N, as shown in Figure 5. This is consistent with the parity-time symmetry, discussed in Reference [22].

10. GENERAL WAVE FIELD REPRESENTATION

Reciprocity theorems interrelate wave fields in two different states [29–31]. Here, we derive a general reciprocity theorem for a homogeneous, time-variant material, which we will use later in this section as the basis for deriving a general wave field representation for this class of materials. To this end, we define

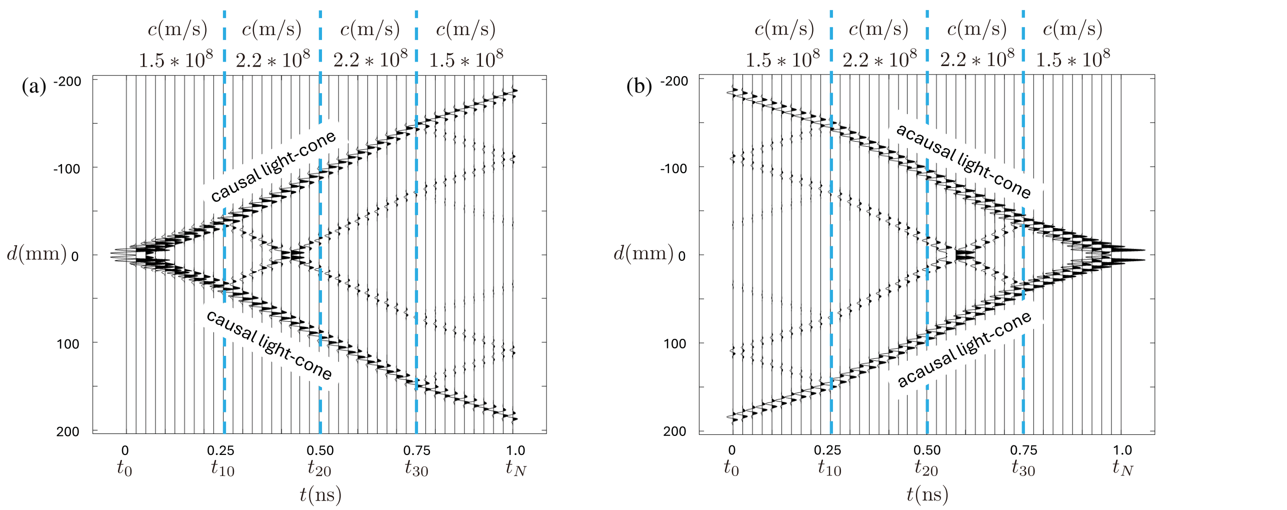

FIGURE 5. Cross-sections along the diagonal $x = z$ of (a) the causal and (b) the acausal Green's function in a symmetric time-variant material.

two independent states, A and B. State A is characterized by time-variant material parameters $\varepsilon_A(t)$ and $\mu_A(t)$, a 6×1 wave field vector $\mathbf{q}_A(\mathbf{x}, t)$, and a 6×1 source vector $\mathbf{d}_A(\mathbf{x}, t)$. State B is characterized similarly, with subscripts A replaced by subscripts B. In the spatial Fourier domain, we have the following matrix-vector wave equations for these two states:

$$\partial_t\check{\mathbf{q}}_A = \check{\mathbf{A}}_A\check{\mathbf{q}}_A + \check{\mathbf{d}}_A, \tag{77}$$

$$\partial_t\check{\mathbf{q}}_B = \check{\mathbf{A}}_B\check{\mathbf{q}}_B + \check{\mathbf{d}}_B, \tag{78}$$

where $\check{\mathbf{q}}_A$, $\check{\mathbf{d}}_A$, $\check{\mathbf{q}}_B$, and $\check{\mathbf{d}}_B$ are the Fourier transforms of $\mathbf{q}_A$, $\mathbf{d}_A$, $\mathbf{q}_B$, and $\mathbf{d}_B$, respectively; $\check{\mathbf{A}}_A$ and $\check{\mathbf{A}}_B$ are defined in Equation (29) with the material parameters of states A and B, respectively.

We evaluate the quantity $\partial_t\{\check{\mathbf{q}}_A^t\mathbf{N}\check{\mathbf{q}}_B\}$, using Equations (77), (78), and (19), which yields

$$\begin{aligned}\partial_t\{\check{\mathbf{q}}_A^t\mathbf{N}\check{\mathbf{q}}_B\} &= \check{\mathbf{q}}_A^t(\check{\mathbf{A}}_A^t\mathbf{N} + \mathbf{N}\check{\mathbf{A}}_B)\check{\mathbf{q}}_B + \check{\mathbf{d}}_A^t\mathbf{N}\check{\mathbf{q}}_B + \check{\mathbf{q}}_A^t\mathbf{N}\check{\mathbf{d}}_B\\ &= \check{\mathbf{q}}_A^t\mathbf{N}(\check{\mathbf{A}}_B - \check{\mathbf{A}}_A)\check{\mathbf{q}}_B + \check{\mathbf{d}}_A^t\mathbf{N}\check{\mathbf{q}}_B + \check{\mathbf{q}}_A^t\mathbf{N}\check{\mathbf{d}}_B.\end{aligned} \tag{79}$$

Integrating both sides from t_0 to t_N (with no specific order of t_0 and t_N), we obtain the following reciprocity theorem

$$\begin{aligned}&\check{\mathbf{q}}_A^t\mathbf{N}\check{\mathbf{q}}_B\Big|_{t_0}^{t_N}\\ &= \int_{t_0}^{t_N}\{\check{\mathbf{q}}_A^t\mathbf{N}(\check{\mathbf{A}}_B - \check{\mathbf{A}}_A)\check{\mathbf{q}}_B + \check{\mathbf{d}}_A^t\mathbf{N}\check{\mathbf{q}}_B + \check{\mathbf{q}}_A^t\mathbf{N}\check{\mathbf{d}}_B\}\mathrm{d}t.\end{aligned} \tag{80}$$

Substituting $\check{\mathbf{q}}$, $\check{\mathbf{d}}$, $\check{\mathbf{A}}$ and $\mathbf{N}$, as defined in Equations (28), (29), and (20), yields

$$\begin{aligned}&-\left(\check{\mathbf{D}}_A^t(i\mathbf{k}\times\check{\mathbf{B}}_B) - (i\mathbf{k}\times\check{\mathbf{B}}_A)^t\check{\mathbf{D}}_B\right)\Big|_{t_0}^{t_N}\\ &= \int_{t_0}^{t_N}\Big(-\Delta\varepsilon\check{\mathbf{D}}_A^t(\mathbf{k}\times\mathbf{k}\times\check{\mathbf{D}}_B) + \Delta\mu(i\mathbf{k}\times\check{\mathbf{B}}_A)^t(i\mathbf{k}\times\check{\mathbf{B}}_B)\\ &\quad+(\check{\mathbf{J}}_A^{\mathrm{e}})^t(i\mathbf{k}\times\check{\mathbf{B}}_B) - (i\mathbf{k}\times\check{\mathbf{J}}_A^{\mathrm{m}})^t\check{\mathbf{D}}_B\\ &\quad+\check{\mathbf{D}}_A^t(i\mathbf{k}\times\check{\mathbf{J}}_B^{\mathrm{m}}) - (i\mathbf{k}\times\check{\mathbf{B}}_A)^t\check{\mathbf{J}}_B^{\mathrm{e}}\Big)\mathrm{d}t,\end{aligned} \tag{81}$$

with

$$\Delta\varepsilon = \frac{1}{\varepsilon_B} - \frac{1}{\varepsilon_A}, \quad \Delta\mu = \frac{1}{\mu_B} - \frac{1}{\mu_A}. \tag{82}$$

Because the products in the $\mathbf{k}, t$-domain correspond to spatial convolutions in the $\mathbf{x}, t$ domain, Equation (81) is a reciprocity theorem of the space-convolution type for a homogeneous, time-variant material. This is the counterpart of the reciprocity theorem of the time-convolution type for an inhomogeneous, time-invariant material [24, Chapter 28.4].

Wave-field representations are obtained by replacing one of the states in a reciprocity theorem by a Green's state [32–34]. Here, we use Equation (81) as the basis for deriving a wave-field representation for a homogeneous, time-variant material. For convenience, we choose identical material parameters in the two states, that is, $\varepsilon_A(t) = \varepsilon_B(t) = \varepsilon(t)$ and $\mu_A(t) = \mu_B(t) = \mu(t)$. For state B, we choose the actual state; hence, we drop the subscript B from the source and wave-field vectors. For state A, we choose a Green's state. To this end, analogous to Section 3, we replace the source vector $-i\mathbf{k}\times\check{\mathbf{J}}_A^{\mathrm{m}}(\mathbf{k}, t)$ by a unit matrix at $t = t'$, that is, $\delta(t - t')\mathbf{I}$, and we set the source vector $\check{\mathbf{J}}_A^{\mathrm{e}}(\mathbf{k}, t)$ to zero. We choose t' between t_0 and t_N, with $t_0 < t' < t_N$. We replace the wave-field vector $\check{\mathbf{D}}_A(\mathbf{k}, t)$ by the acausal Green's matrix $\check{\boldsymbol{\mathcal{G}}}^a(\mathbf{k}, \mathbf{0}, t, t')$, with $\check{\boldsymbol{\mathcal{G}}}^a(\mathbf{k}, \mathbf{0}, t, t') = \mathbf{O}$ for $t > t'$. With this choice for the Green's matrix, the matrix $\delta(t - t')\mathbf{I}$ represents a sink. The wave-field vector $i\mathbf{k}\times\check{\mathbf{B}}_A$ is, according to the spatial Fourier transform of Equation (5), identical to $\mu(t)\partial_t\check{\mathbf{D}}_A(\mathbf{k}, t)$. Hence, we replace $i\mathbf{k}\times\check{\mathbf{B}}_A$ by $\mu(t)\partial_t\check{\boldsymbol{\mathcal{G}}}^a(\mathbf{k}, \mathbf{0}, t, t')$. Substituting these choices for states A and B into Equation (81), using $\{\check{\boldsymbol{\mathcal{G}}}^a(\mathbf{k}, \mathbf{0}, t, t')\}^t = \check{\boldsymbol{\mathcal{G}}}(\mathbf{k}, \mathbf{0}, t', t)$ (Equation (71)), with causality condition $\check{\boldsymbol{\mathcal{G}}}(\mathbf{k}, \mathbf{0}, t', t) = \mathbf{O}$ for $t > t'$, we obtain

$$\begin{aligned}\check{\mathbf{D}}(\mathbf{k}, t') &= \check{\boldsymbol{\mathcal{G}}}(\mathbf{k}, \mathbf{0}, t', t_0)\left(i\mathbf{k}\times\check{\mathbf{B}}(\mathbf{k}, t_0)\right)\\ &\quad-\left(\mu(t_0)\partial_{t_0}\check{\boldsymbol{\mathcal{G}}}(\mathbf{k}, \mathbf{0}, t', t_0)\right)\check{\mathbf{D}}(\mathbf{k}, t_0)\\ &\quad-\int_{t_0}^{t'}\Big(\check{\boldsymbol{\mathcal{G}}}(\mathbf{k}, \mathbf{0}, t', t)\left(i\mathbf{k}\times\check{\mathbf{J}}^{\mathrm{m}}(\mathbf{k}, t)\right)\end{aligned}$$

$$-\left(\mu(t)\partial_t\check{\boldsymbol{\mathcal{G}}}(\mathbf{k},\mathbf{0},t',t)\right)\check{\mathbf{J}}^{\mathrm{e}}(\mathbf{k},t)\Big)\mathrm{d}t \qquad (83)$$

(Note that the integration boundary t_N in Equation (81) has been replaced by t' due to the causality condition of the Green's function). Equation (83) is a representation in the spatial Fourier domain of the electric flux density in a homogeneous, time-variant material at time instant t', in terms of the initial magnetic and electric flux densities at t_0, supplemented with contributions from sources between t_0 and t'. It is the counterpart of the classical representation in the temporal Fourier domain of the electric field strength in an inhomogeneous, time-invariant material at position $\mathbf{x}'$, in terms of the magnetic and electric field strengths at a boundary enclosing $\mathbf{x}'$, supplemented with contributions from sources inside the enclosing boundary [35, Chapter 8.14] and [24, Chapter 28.12]. In the absence of sources inside the enclosing boundary, this classical representation reduces to an integral along the enclosing boundary (known as the Kirchhoff integral), quantifying Huygens' principle. Similarly, in the absence of sources between t_0 and t', Equation (83) reduces to the first two terms, expressing the electric flux density at t' in terms of the initial magnetic and electric flux densities at t_0.

Finally, we transform the representation of Equation (83) back to the space-time domain, using Equation (26), with $\mathbf{x}$ and t replaced by $\mathbf{x}'$ and t'. Using the shift-invariance of the Green's matrix (Equation (15)), we obtain

$$\begin{aligned}\mathbf{D}(\mathbf{x}',t') &= \int_{\mathbb{R}^3}\Big(\boldsymbol{\mathcal{G}}(\mathbf{x}',\mathbf{x},t',t_0)\,(\boldsymbol{\nabla}\times\mathbf{B}(\mathbf{x},t_0))\\ &\quad-\left(\mu(t_0)\partial_{t_0}\boldsymbol{\mathcal{G}}(\mathbf{x}',\mathbf{x},t',t_0)\right)\mathbf{D}(\mathbf{x},t_0)\Big)\mathrm{d}^3\mathbf{x}\\ &\quad-\int_{t_0}^{t'}\int_{\mathbb{R}^3}\Big(\boldsymbol{\mathcal{G}}(\mathbf{x}',\mathbf{x},t',t)\,(\boldsymbol{\nabla}\times\mathbf{J}^{\mathrm{m}}(\mathbf{x},t))\\ &\quad-\left(\mu(t)\partial_t\boldsymbol{\mathcal{G}}(\mathbf{x}',\mathbf{x},t',t)\right)\mathbf{J}^{\mathrm{e}}(\mathbf{x},t)\Big)\mathrm{d}^3\mathbf{x}\mathrm{d}t. \qquad (84)\end{aligned}$$

From this representation, we observe that the initial wave fields (at t_0) and sources (between t_0 and t') in the whole of $\mathbb{R}^3$ contribute to the electric flux density $\mathbf{D}(\mathbf{x}',t')$.

11. GREEN'S MATRIX RETRIEVAL

For inhomogeneous, time-invariant materials, it has been shown that the Green's function between two positions in space can, under specific conditions, be retrieved from the time correlation of wave field observations at those positions [36–43]. Here, we derive an expression for retrieving the 3D electromagnetic Green's matrix between two time instants in a homogeneous, time-variant material.

We start with the following special case of Equation (44)

$$\check{\mathbf{W}}(\mathbf{k},t',t)=\check{\mathbf{W}}(\mathbf{k},t',t_0)\check{\mathbf{W}}(\mathbf{k},t_0,t), \qquad (85)$$

with the propagator matrices expressed in terms of homogeneous Green's matrices, as in Equation (70). We choose $t_0 < t'$ and $t_0 < t$, but the order of t and t' is arbitrary. With these choices, the homogeneous Green's matrices in $\check{\mathbf{W}}(\mathbf{k},t',t_0)$ are reduced to causal Green's matrices, whereas those in $\check{\mathbf{W}}(\mathbf{k},t_0,t)$ are reduced to acausal Green's matrices. To turn Equation (85) into an expression with only causal Green's matrices on the right-hand side, we apply the symmetry relation of Equation (47) to $\check{\mathbf{W}}(\mathbf{k},t_0,t)$. Thus, Equation (85) becomes

$$\check{\mathbf{W}}(\mathbf{k},t',t)=\check{\mathbf{W}}(\mathbf{k},t',t_0)\mathbf{N}^{-1}\check{\mathbf{W}}^t(\mathbf{k},t,t_0)\mathbf{N}. \qquad (86)$$

According to Equation (70), the upper-right element of $\check{\mathbf{W}}(\mathbf{k},t',t)$ equals $-\check{\boldsymbol{\mathcal{G}}}^h(\mathbf{k},\mathbf{0},t',t)$. From Equation (86), we obtain the following expression for this matrix:

$$\begin{aligned}&\check{\boldsymbol{\mathcal{G}}}^h(\mathbf{k},\mathbf{0},t',t)\\ &= \mu(t_0)\Big(\{\partial_{t_0}\check{\boldsymbol{\mathcal{G}}}(\mathbf{k},\mathbf{0},t',t_0)\}\{\check{\boldsymbol{\mathcal{G}}}(\mathbf{k},\mathbf{0},t,t_0)\}^t\\ &\quad-\check{\boldsymbol{\mathcal{G}}}(\mathbf{k},\mathbf{0},t',t_0)\{\partial_{t_0}\check{\boldsymbol{\mathcal{G}}}(\mathbf{k},\mathbf{0},t,t_0)\}^t\Big). \qquad (87)\end{aligned}$$

From Equation (58) it follows that $\check{\boldsymbol{\mathcal{G}}}(\mathbf{k},\mathbf{0},t,t_0)$ is symmetric in $\mathbf{k}$, that is, $\check{\boldsymbol{\mathcal{G}}}(\mathbf{k},\mathbf{0},t,t_0)=\check{\boldsymbol{\mathcal{G}}}(-\mathbf{k},\mathbf{0},t,t_0)$. Using this in Equation (87) and transforming the resulting expression back to the space-time domain, we obtain:

$$\begin{aligned}&\boldsymbol{\mathcal{G}}^h(\mathbf{x}',\mathbf{0},t',t)\\ &= \mu(t_0)\int_{\mathbb{R}^3}\Big(\{\partial_{t_0}\boldsymbol{\mathcal{G}}(\mathbf{x}'+\mathbf{x},\mathbf{0},t',t_0)\}\{\boldsymbol{\mathcal{G}}(\mathbf{x},\mathbf{0},t,t_0)\}^t\\ &\quad-\boldsymbol{\mathcal{G}}(\mathbf{x}'+\mathbf{x},\mathbf{0},t',t_0)\{\partial_{t_0}\boldsymbol{\mathcal{G}}(\mathbf{x},\mathbf{0},t,t_0)\}^t\Big)\mathrm{d}^3\mathbf{x}. \qquad (88)\end{aligned}$$

The two terms on the right-hand side of this equation represent 3D space correlations of wave fields, observed at time instants t and t', in response to a source and its derivative at $\mathbf{x}=\mathbf{0}$ and $t=t_0$. The left-hand side is the homogeneous Green's matrix between these time instants. Hence, this is the sought expression for retrieving Green's matrix in a homogeneous, time-variant material.

It should be noted that in practical situations, the Green's matrices on the right-hand side of Equation (88) will only be available within a finite aperture. Moreover, some components of the matrices may not be available, the remaining components may be contaminated by noise, etc. Hence, in practice, retrieving the Green's matrix of a homogeneous, time-variant material involves several approximations. This is comparable with Green's function retrieval in inhomogeneous, time-invariant materials, where in practice, the retrieved Green's function is also an approximation. Much research has been done to overcome limitations of practical Green's function retrieval, such as iterative correlation [44], multidimensional deconvolution [45, 46], and directional balancing [47]. To improve the quality of the retrieved Green's matrix in homogeneous, time-variant material in practical situations, modifications of Equation (88) require further research, beyond the scope of this paper.

12. CONCLUSIONS

We have derived several fundamental properties and relations for 3D electromagnetic wave propagation and scattering in a homogeneous, time-variant material. Starting with the Maxwell equations, we arrived at a second-order wave equation, following the same procedure as in References [20–22] (Section 2). Unlike the usual wave equation for a classical time-invariant material, which governs the electric field strength $\mathbf{E}(\mathbf{x},t)$, the field vector in the wave equation for a homogeneous, time-variant material is the electric flux density $\mathbf{D}(\mathbf{x},t)$.

By replacing the 3×1 source vector in the wave equation with a 3×3 unit source matrix at $\mathbf{x}=\mathbf{x}_0$ and $t=t_0$, we obtained a wave equation for the 3×3 Green's matrix $\boldsymbol{\mathcal{G}}(\mathbf{x},\mathbf{x}_0,t,t_0)$ (Section 3). We specified a causality condition for this Green's matrix to ensure that it is the causal response to the source at $\mathbf{x}=\mathbf{x}_0$ and $t=t_0$. We also introduced an acausal Green's matrix $\boldsymbol{\mathcal{G}}^a(\mathbf{x},\mathbf{x}_0,t,t_0)$, obeying the same wave equation but with an acausality condition, for which the singularity at $\mathbf{x}=\mathbf{x}_0$ and $t=t_0$ acts as a sink (instead of a source). Unlike in a time-invariant material, where the acausal Green's function is the time-reversal of the causal Green's function, this relation does not (in general) hold for the causal and acausal Green's matrices in a time-variant material.

We derived a matrix-vector wave equation for a 6×1 wave field vector $\mathbf{q}(\mathbf{x},t)$, containing electric and magnetic flux densities $\mathbf{D}(\mathbf{x},t)$ and $\mathbf{B}(\mathbf{x},t)$ (Section 4). There are several ways to define the 6×6 operator matrix $\mathbf{A}(t)$ in this equation. We argued that the most obvious form of $\mathbf{A}(t)$ (Equation (17)) does not obey the symmetry property required to establish the fundamental properties of wave propagation and scattering in a time-variant material. We chose an alternative form of $\mathbf{A}(t)$ (Equation (23)), which obeys the required symmetry. Hand-in-hand with this choice, we replaced $\mathbf{B}$ in the wave field vector $\mathbf{q}$ by $-\boldsymbol{\nabla}\times\mathbf{B}$ (Equation (22)). For the latter choice of the wave field vector $\mathbf{q}$, we showed that $\check{\mathbf{q}}^\dagger\mathbf{N}\check{\mathbf{q}}$ (where $\check{\mathbf{q}}$ is the 3D spatial Fourier transform of $\mathbf{q}$) is proportional to the net momentum density $\check{M}(\mathbf{k},t)$ (Section 5). Using the symmetry of the operator matrix $\check{\mathbf{A}}$, we showed that the net momentum density $\check{M}(\mathbf{k},t)$ is conserved (that is, independent of t) in a source-free, piecewise, continuous, time-variant material. This is consistent with [22].

By replacing the 6×1 wave field vector $\check{\mathbf{q}}(\mathbf{k},t)$ in the matrix-vector wave equation by a 6×6 propagator matrix $\check{\mathbf{W}}(\mathbf{k},t,t_0)$ (and setting the source term to zero), we obtained the wave equation for this matrix (Section 6). We specified the initial condition $\check{\mathbf{W}}(\mathbf{k},t_0,t_0)=\mathbf{I}$. For variable t, the expression $\check{\mathbf{W}}(\mathbf{k},t,t_0)\check{\mathbf{q}}(\mathbf{k},t_0)$ "propagates" the wave field vector $\check{\mathbf{q}}(\mathbf{k},t_0)$ from t_0 through the time-variant material to t .

Using the symmetry of the operator matrix $\check{\mathbf{A}}$, we derived symmetry properties of the propagator matrix (Section 7). We showed that the upper-right 3×3 submatrix of the propagator matrix equals the acausal Green's matrix, minus the causal Green's matrix (Section 8). Using this equality and symmetry of the propagator matrix, we derived a relation between the causal and acausal Green's matrices (Section 9). We illustrated a selection of components of the causal and acausal Green's matrices with numerical examples. The direct outward propagating waves of the causal Green's function form a "causal light-cone," diverging from the source at t_0 (Figures 1 and 2), and the direct inward propagating waves of the acausal Green's function form an "acausal light-cone," converging to a sink at t_N (Figures 3 and 4). In both cases, all the scattered events reside inside these cones. The causal Green's function, observed at t_N, equals the acausal Green's function, observed at t_0. For all other time instants between t_0 and t_N, there is no apparent relationship between the causal and acausal Green's functions, except when the time-variant material between t_0 and t_N is symmetric (Figure 5), the latter being consistent with the parity-time symmetry, discussed in Reference [22].

Using the matrix-vector wave equation, the symmetry property of the operator matrix $\check{\mathbf{A}}$, and the relation between the causal and acausal Green's matrices, we obtained a representation of the electric flux density in a homogeneous, time-variant material at time instant t', in terms of the initial magnetic and electric flux densities at t_0, plus contributions from sources between t_0 and t' (Section 10). This is the counterpart of the classical representation of the electric field strength in an inhomogeneous, time-invariant material at position $\mathbf{x}'$, in terms of the magnetic and electric field strengths at a boundary enclosing $\mathbf{x}'$ (the Kirchhoff integral), plus contributions from sources inside the enclosing boundary.

Using the symmetry of the propagator matrix and the relation between its upper-right 3×3 submatrix and the causal and acausal Green's matrices, we derived an expression for retrieving the Green's matrix between t and t' in a homogeneous, time-variant material, from 3D space correlations of wave field observations at t and t' (Section 11). This is the counterpart of an expression for retrieving the Green's function between $\mathbf{x}$ and $\mathbf{x}'$ in an inhomogeneous, time-invariant material, from 1D time correlations of wave field observations at $\mathbf{x}$ and $\mathbf{x}'$.

We restricted the analysis in this study to waves in time-variant materials, whose parameters are constant in space. The behavior of waves in materials with parameters that vary with space and time has been analyzed for several special cases of 1D and 2D materials [7, 10, 13, 15]. A more general analysis is complicated by the fact that waves in inhomogeneous materials are preferably described in terms of the field strengths $\mathbf{E}$ and $\mathbf{H}$, whereas the flux densities $\mathbf{D}$ and $\mathbf{B}$ are the preferred quantities to describe waves in time-variant materials. In particular, at spatial boundaries the field strengths $\mathbf{E}$ and $\mathbf{H}$ are continuous, and the flux densities $\mathbf{D}$ and $\mathbf{B}$ are continuous at time boundaries. A general theory for wave propagation and scattering in 3D arbitrarily inhomogeneous, time-variant materials should account simultaneously for the specific behaviors of field strengths and flux densities. This remains a subject of investigation.

APPENDIX A. PROPAGATOR MATRIX FOR A TIME-INDEPENDENT SLAB

For a time-independent slab between t_{n-1} and t_n, matrix $\check{\mathbf{A}}_n$, defined in Equation (29) with constant material parameters ε_n and μ_n, is time-independent. For this situation, the solution of

Equation (39), with the initial condition of Equation (40) (with t_0 replaced by t_{n-1}), can be formally written as

$$\check{\mathbf{W}}(\mathbf{k}, t_n, t_{n-1}) = \exp\{\check{\mathbf{A}}_n \Delta t_n\}, \tag{A1}$$

with $\Delta t_n = t_n - t_{n-1}$. We expand the exponential in Equation (A1) as follows

$$\check{\mathbf{W}}(\mathbf{k}, t_n, t_{n-1}) = \mathbf{I} + \frac{\check{\mathbf{A}}_n \Delta t_n}{1!} + \frac{(\check{\mathbf{A}}_n \Delta t_n)^2}{2!} + \frac{(\check{\mathbf{A}}_n \Delta t_n)^3}{3!} + \cdots . \tag{A2}$$

We thus find

$$\check{\mathbf{W}}(\mathbf{k}, t_n, t_{n-1}) = \begin{pmatrix} \check{\mathbf{W}}^{D,D} & \check{\mathbf{W}}^{D,B} \\ \check{\mathbf{W}}^{B,D} & \check{\mathbf{W}}^{B,B} \end{pmatrix} (\mathbf{k}, t_n, t_{n-1}), \tag{A3}$$

with

$$\check{\mathbf{W}}^{D,D} = \check{\mathbf{W}}^{B,B} = \frac{1}{k_r^2} \begin{pmatrix} (k_y^2 + k_z^2)\cos\phi_n + k_x^2 & -k_x k_y(\cos\phi_n - 1) & -k_x k_z(\cos\phi_n - 1) \\ -k_x k_y(\cos\phi_n - 1) & (k_x^2 + k_z^2)\cos\phi_n + k_y^2 & -k_y k_z(\cos\phi_n - 1) \\ -k_x k_z(\cos\phi_n - 1) & -k_y k_z(\cos\phi_n - 1) & (k_x^2 + k_y^2)\cos\phi_n + k_z^2 \end{pmatrix}, \tag{A4}$$

$$\check{\mathbf{W}}^{D,B} = \frac{-1}{\mu_n c_n k_r^3} \begin{pmatrix} (k_y^2 + k_z^2)\sin\phi_n + k_x^2\phi_n & -k_x k_y(\sin\phi_n - \phi_n) & -k_x k_z(\sin\phi_n - \phi_n) \\ -k_x k_y(\sin\phi_n - \phi_n) & (k_x^2 + k_z^2)\sin\phi_n + k_y^2\phi_n & -k_y k_z(\sin\phi_n - \phi_n) \\ -k_x k_z(\sin\phi_n - \phi_n) & -k_y k_z(\sin\phi_n - \phi_n) & (k_x^2 + k_y^2)\sin\phi_n + k_z^2\phi_n \end{pmatrix}, \tag{A5}$$

$$\check{\mathbf{W}}^{B,D} = \frac{\mu_n c_n}{k_r} \begin{pmatrix} (k_y^2 + k_z^2)\sin\phi_n & -k_x k_y \sin\phi_n & -k_x k_z \sin\phi_n \\ -k_x k_y \sin\phi_n & (k_x^2 + k_z^2)\sin\phi_n & -k_y k_z \sin\phi_n \\ -k_x k_z \sin\phi_n & -k_y k_z \sin\phi_n & (k_x^2 + k_y^2)\sin\phi_n \end{pmatrix}, \tag{A6}$$

where ϕ_n, c_n, and k_r are defined as

$$\phi_n = k_r c_n \Delta t_n, \quad c_n = \frac{1}{\sqrt{\mu_n \varepsilon_n}},$$

$$k_r = |\mathbf{k}| = \sqrt{k_x^2 + k_y^2 + k_z^2}. \tag{A7}$$

REFERENCES

[1] Morgenthaler, F. R., "Velocity modulation of electromagnetic waves," *IRE Transactions on Microwave Theory and Techniques*, Vol. 6, No. 2, 167–172, 1958.

[2] Jiang, C.-L., "Wave propagation and dipole radiation in a suddenly created plasma," *IEEE Transactions on Antennas and Propagation*, Vol. 23, No. 1, 83–90, 1975.

[3] Mendonça, J. T. and P. K. Shukla, "Time refraction and time reflection: Two basic concepts," *Physica Scripta*, Vol. 65, No. 2, 160–163, 2002.

[4] Koutserimpas, T. T. and R. Fleury, "Electromagnetic waves in a time periodic medium with step-varying refractive index," *IEEE Transactions on Antennas and Propagation*, Vol. 66, No. 10, 5300–5307, 2018.

[5] Caloz, C. and Z.-L. Deck-Léger, "Spacetime metamaterials — Part I: General concepts," *IEEE Transactions on Antennas and Propagation*, Vol. 68, No. 3, 1569–1582, 2020.

[6] Ramaccia, D., A. Toscano, and F. Bilotti, "Light propagation through metamaterial temporal slabs: Reflection, refraction, and special cases," *Optics Letters*, Vol. 45, No. 20, 5836–5839, 2020.

[7] Apffel, B. and E. Fort, "Frequency conversion cascade by crossing multiple space and time interfaces," *Physical Review Letters*, Vol. 128, No. 6, 064501, 2022.

[8] Moussa, H., G. Xu, S. Yin, E. Galiffi, Y. Ra'di, and A. Alù, "Observation of temporal reflection and broadband frequency translation at photonic time interfaces," *Nature Physics*, Vol. 19, No. 6, 863–868, 2023.

[9] Pacheco-Peña, V., M. Fink, and N. Engheta, "Temporal chirp, temporal lensing, and temporal routing via space-time interfaces," *Physical Review B*, Vol. 111, No. 10, L100306, 2025.

[10] Stefanini, L., E. Galiffi, S. Yin, S. Singh, D. M. Solís, N. Engheta, A. Toscano, D. Ramaccia, F. Bilotti, and A. Alù, "Theory and experimental observation of scattering by a space-time corner," *Physical Review Letters*, Vol. 135, No. 11, 113802, 2025.

[11] Xiao, Y., D. N. Maywar, and G. P. Agrawal, "Reflection and transmission of electromagnetic waves at a temporal boundary," *Optics Letters*, Vol. 39, No. 3, 574–577, 2014.

[12] Salem, M. A. and C. Caloz, "Space-time cross-mapping and application to wave scattering," *arXiv preprint arXiv:1504.02012*, 2015.

[13] Caloz, C. and Z.-L. Deck-Léger, "Spacetime metamaterials — Part II: Theory and applications," *IEEE Transactions on Antennas and Propagation*, Vol. 68, No. 3, 1583–1598, 2020.

[14] Wapenaar, K., J. Aichele, and D.-J. van Manen, "Waves in space-dependent and time-dependent materials: A systematic comparison," *Wave Motion*, Vol. 130, 103374, 2024.

[15] Van Manen, D.-J., J. Aichele, J. Müller, M. Serra-Garcia, and K. Wapenaar, "On acoustic space-time media that compute their own inverse," *arXiv preprint arXiv:2406.15203*, 2024.

[16] Koutserimpas, T. T., "Wake-tail effects in two-dimensional wave refocusing," *Physical Review E*, Vol. 113, No. 6, 065102, 2026.

[17] Pacheco-Peña, V. and N. Engheta, "Effective medium concept in temporal metamaterials," *Nanophotonics*, Vol. 9, No. 2, 379–391, 2020.

[18] Štumpf, M., F. Loreto, G. Antonini, and J. Ekman, "Pulsed wave propagation along a transmission line with time-varying wavespeed," *IEEE Microwave and Wireless Technology Letters*, Vol. 33, No. 7, 963–966, 2023.

[19] Wapenaar, K., "Green's functions, propagation invariants, reciprocity theorems, wave-field representations and propagator matrices in two-dimensional time-dependent materials," *Proceedings of the Royal Society A*, Vol. 481, No. 2307, 20240479, 2025.

[20] Budko, N. V., "Electromagnetic radiation in a time-varying background medium," *Physical Review A*, Vol. 80, No. 5,

053817, 2009.

[21] De Hoop, A. T. and I. E. Lager, "Closed-form analytic expressions for the pulsed-source radiated electromagnetic field in a class of media with time-varying wave speed," *Wave Motion*, Vol. 51, No. 3, 418–424, 2014.

[22] Koutserimpas, T. T. and R. Fleury, "Electromagnetic fields in a time-varying medium: Exceptional points and operator symmetries," *IEEE Transactions on Antennas and Propagation*, Vol. 68, No. 9, 6717–6724, 2020.

[23] Landau, L. D. and E. M. Lifshitz, *Electrodynamics of Continuous Media*, Pergamon Press, 1960.

[24] De Hoop, A. T., *Handbook of Radiation and Scattering of Waves*, Academic Press, London, 1995.

[25] Torrent, D., W. J. Parnell, and A. N. Norris, "Loss compensation in time-dependent elastic metamaterials," *Physical Review B*, Vol. 97, No. 1, 014105, 2018.

[26] Stumpf, M. and G. Antonini, "State-variable analysis of pulsed EM-fields in temporally layered media," *Scientific Reports*, 2026.

[27] Feynman, R., R. Leighton, and M. Sands, *The Feynman Lectures on Physics, Volume II*, California Institute of Technology, 1963.

[28] Burns, L., K. Y. Bliokh, F. Nori, and J. Dressel, "Acoustic versus electromagnetic field theory: Scalar, vector, spinor representations and the emergence of acoustic spin," *New Journal of Physics*, Vol. 22, No. 5, 053050, 2020.

[29] Lorentz, H. A., "The theorem of Poynting concerning the energy in the electromagnetic field and two general propositions concerning the propagation of light," *Koninklijke Akademie van Wetenschappen*, Vol. 4, 176–187, 1895.

[30] Knopoff, L. and A. F. Gangi, "Seismic reciprocity," *Geophysics*, Vol. 24, No. 4, 681–691, 1959.

[31] De Hoop, A. T., "Time-domain reciprocity theorems for electromagnetic fields in dispersive media," *Radio Science*, Vol. 22, No. 7, 1171–1178, 1987.

[32] Knopoff, L., "Diffraction of elastic waves," *The Journal of the Acoustical Society of America*, Vol. 28, No. 2, 217–229, 1956.

[33] De Hoop, A. T., "Representation theorems for the displacement in an elastic solid and their application to elastodynamic diffraction theory," Ph.D. dissertation, Delft University of Technology, Delft, The Netherlands, 1958.

[34] Gangi, A. F., "A derivation of the seismic representation theorem using seismic reciprocity," *Journal of Geophysical Research*, Vol. 75, No. 11, 2088–2095, 1970.

[35] Stratton, J. A., *Electromagnetic Theory*, McGraw-Hill, New York, 1941.

[36] Weaver, R. L. and O. I. Lobkis, "Ultrasonics without a source: Thermal fluctuation correlations at MHz frequencies," *Physical Review Letters*, Vol. 87, No. 13, 134301, 2001.

[37] Campillo, M. and A. Paul, "Long-range correlations in the diffuse seismic coda," *Science*, Vol. 299, No. 5606, 547–549, 2003.

[38] Wapenaar, K., "Synthesis of an inhomogeneous medium from its acoustic transmission response," *Geophysics*, Vol. 68, No. 5, 1756–1759, 2003.

[39] Snieder, R., "Extracting the Green's function from the correlation of coda waves: A derivation based on stationary phase," *Physical Review E*, Vol. 69, 046610, 2004.

[40] Malcolm, A. E., J. A. Scales, and B. A. van Tiggelen, "Extracting the Green function from diffuse, equipartitioned waves," *Physical Review E*, Vol. 70, 015601, 2004.

[41] Roux, P. and W. A. Kuperman, "Extracting coherent wave fronts from acoustic ambient noise in the ocean," *The Journal of the Acoustical Society of America*, Vol. 116, No. 4, 1995–2003, 2004.

[42] Slob, E., D. Draganov, and K. Wapenaar, "Interferometric electromagnetic Green's functions representations using propagation invariants," *Geophysical Journal International*, Vol. 169, No. 1, 60–80, 2007.

[43] Slob, E. C. and K. Wapenaar, "Retrieving the Green's function from cross correlation in a bianisotropic medium," *Progress In Electromagnetics Research*, Vol. 93, 255–274, 2009.

[44] Stehly, L., M. Campillo, B. Froment, and R. L. Weaver, "Reconstructing Green's function by correlation of the coda of the correlation (C^3) of ambient seismic noise," *Journal of Geophysical Research: Solid Earth*, Vol. 113, No. B11, 2008.

[45] Wapenaar, K. and J. van der Neut, "A representation for Green's function retrieval by multidimensional deconvolution," *The Journal of the Acoustical Society of America*, Vol. 128, No. 6, EL366–EL371, 2010.

[46] Van der Neut, J., J. Thorbecke, K. Mehta, E. Slob, and K. Wapenaar, "Controlled-source interferometric redatuming by cross-correlation and multidimensional deconvolution in elastic media," *Geophysics*, Vol. 76, No. 4, SA63–SA76, 2011.

[47] Curtis, A. and D. Halliday, "Directional balancing for seismic and general wavefield interferometry," *Geophysics*, Vol. 75, No. 1, SA1–SA14, 2010.